remote sensing

MDPI

Review

Monitoring Wildfire Risk with a Near-Real-Time Live Fuel Moisture Content System: A Review and Roadmap for Operational Application in New Zealand

Michael S. Watt [1,*], Shana Gross [1], John Keithley Difuntorum [2], Jessica L. McCarty [3], H. Grant Pearce [4], Jacquelyn K. Shuman [3] and Marta Yebra [5,6]

[1] Scion Group, Bioeconomy Science Institute, 10 Kyle Street, Riccarton, Christchurch 8440, New Zealand; shana.gross@scionresearch.com
[2] School of Earth and Environment, University of Canterbury, Ilam, Christchurch 8041, New Zealand; jldifuntorum@gmail.com
[3] Earth Science Division, NASA Ames Research Center, Moffett Field, CA 94035, USA; jessica.l.mccarty-kern@nasa.gov (J.L.M.); jacquelyn.k.shuman@nasa.gov (J.K.S.)
[4] Fire and Emergency New Zealand, Fire Engineering Facility, 79 Creyke Road, Ilam, Christchurch 8041, New Zealand; grant.pearce2@fireandemergency.nz
[5] Fenner School of Environment & Society, Australian National University, Canberra, ACT 2601, Australia; marta.yebra@anu.edu.au
[6] School of Engineering, Australian National University, Canberra, ACT 2601, Australia
* Correspondence: michael.watt@scionresearch.com

Highlights

What are the main findings?

- A comprehensive evaluation of multispectral, hyperspectral, thermal, and mi-crowave sensors, undertaken individually and in combination, shows how LFMC and fuel types can be monitored with specific applicability to New Zealand.
- The review clarifies trade-offs (resolution, cadence, spectral sensitivity), outlines limitations and identifies opportunities to improve mapping of LFMC and fuel type.

What are the implications of the main findings?

- The synthesis provides the technical groundwork for an operational, near-real-time LFMC prediction system in New Zealand with relevance to other fire-prone regions.
- Such a system will enable more reliable, timely wildfire risk assessment and strengthen decision-making for fire management and emergency response.

Abstract

Live fuel moisture content (LFMC) is a critical variable influencing wildfire behavior, ignition potential, and suppression difficulty, yet it remains challenging to monitor consistently across landscapes due to sparse field observations, rapid temporal changes, and vegetation heterogeneity. This study presents a comprehensive review of satellite-based approaches for estimating LFMC, with emphasis on methods applicable to New Zealand, where wildfire risk is increasing due to climate change. We assess the suitability of different remote sensing data sources, including multispectral, thermal, and microwave sensors, and evaluate their integration for characterizing both LFMC and fuel types. Particular attention is given to the trade-offs between data resolution, revisit frequency, and spectral sensitivity. As knowledge of fuel type and structure is critical for understanding wildfire behavior and LFMC, the review also outlines key limitations in existing land cover products for fuel classification and highlights opportunities for improving fuel mapping using remotely sensed data. This review lays the groundwork for the development of an operational LFMC prediction

check for updates

Academic Editor: Xiaoyang Zhang

Received: 25 September 2025
Revised: 21 October 2025
Accepted: 26 October 2025
Published: 29 October 2025

Citation: Watt, M.S.; Gross, S.; Difuntorum, J.K.; McCarty, J.L.; Pearce, H.G.; Shuman, J.K.; Yebra, M. Monitoring Wildfire Risk with a Near-Real-Time Live Fuel Moisture Content System: A Review and Roadmap for Operational Application in New Zealand. *Remote Sens.* **2025**, *17*, 3580. https://doi.org/10.3390/rs17213580

Copyright: © 2025 by the authors. Licensee MDPI, Basel, Switzerland. This article is an open access article distributed under the terms and conditions of the Creative Commons Attribution (CC BY) license (https://creativecommons.org/licenses/by/4.0/).

system in New Zealand, with broader relevance to fire-prone regions globally. Such a system would support real-time wildfire risk assessment and enhance decision-making in fire management and emergency response.

Keywords: fuel type; fire danger; fire risk; HLS; live fuel moisture content; machine learning; radiative transfer models; remote sensing; spectral indices; wildfire

1. Introduction

Climate change is increasing vegetative drought stress and wildfire danger across the globe. Regions that are characterized by dry conditions, such as Australia, the Mediterranean and western North America, have always been prone to forest fires [1,2]. However, human-induced climate change is likely to increase fire activity globally in areas that were less affected in the past [3–5], such as New Zealand [6]. Across New Zealand the number of days with very high and extreme fire danger is projected to increase over baseline conditions by 71% to 2040 and by a further 12% by 2090 [6], with evidence suggesting that this trend has already started in many regions within New Zealand [7]. The mountainous and highly dissected terrain within New Zealand poses additional challenges for fire control, as it creates multiple microclimates, limits accessibility [8], and fire spread has been shown to accelerate on steeper slopes [9].

Effective preparation for future wildfires requires accurate, up-to-date data on all key components of the fire environment including weather, topography, and fuel characteristics [10]. As with many countries, New Zealand has comprehensive information describing topography and temporal and spatial changes in weather. However, appropriately scaled spatial and temporal data on fuels does not currently exist. Vegetative fuel is the material that ignites and burns in a fire, including both live and dead combustible materials of plants, foliage, wood material, litter and organic layers. Fuel moisture content (FMC), defined as the ratio of water present in the fuel to its total dry mass, is one of the most important fuel characteristics for assessing wildfire risk.

Fuel moisture content is commonly divided into dead (DFMC) and live (LFMC) components [11]. Dead fuel moisture content influences the energy and time needed to vaporize moisture before fuels can ignite [12], thereby playing a critical role in determining fire ignition, intensity, rate of spread, and overall fire extent [13]. DFMC is commonly calculated for surface fuels using weather variables and fuel size. While most wildfire risk assessments rely on proxy measures to incorporate DFMC, these proxies often fail to capture the transition potential from surface to crown fires. Moreover, they generally do not account for the spatial heterogeneity and temporal dynamics of fuel moisture—particularly when based on data from an individual weather station. As a result, their predictive capacity for fire behavior and spread intensity is limited to surface fire spread and ignition susceptibility derived from a single weather station, without accounting for topography, microclimate, or rapid short-term weather fluctuations.

Although LFMC is potentially more difficult to quantify, an understanding of spatial and temporal variation in LFMC could greatly improve fire behavior predictions. LFMC has been identified as a key factor influencing ignition timing [14,15], and numerous studies have demonstrated the utility of LFMC thresholds which strongly influence fire occurrence, spread, and area burned [12,16–22]. However, LFMC is highly variable across space and time, and its interpretation requires knowledge of fuel type, making landscape-scale quantification a challenge.

Traditionally, both DFMC and LFMC have been estimated through field measurements [23]. While these methods provide relatively accurate data, they are highly localized, labor-intensive, and time-consuming, making large-scale or long-term monitoring unfeasible [11]. Meteorological data and satellite imagery have been used as an alternative to overcome the spatial and temporal limitations of ground-based sampling [11,24–26]. However, sparse meteorological station coverage often necessitates interpolation, introducing significant computational errors. While weather forecasting models used to predict DFMC help address spatial limitations, they are still constrained by uncertainties, and in particular, prediction of precipitation. However, the meteorological data-based estimation of LFMC is challenging as plants with live fuels have multiple drought adaptation strategies [27]. Although standalone systems have been created, such as the Australian Flammability Monitoring System we are unaware of any country that operationally integrates satellite estimates of LFMC into wildfire risk assessments.

In New Zealand, wildfire hazard is assessed using the New Zealand Fire Danger Rating System (NZFDRS), which is based on the Canadian Fire Danger System (CFFDRS) [28]. The NZFDRS output includes fire danger ratings which categorize wildfire risk. There are four subsystems within the NZFDRS (Figure 1): the Fire Weather Index (FWI) system, the Fire Behavior Prediction (FBP) system, the Fire Occurrence Prediction (FOP) system, and the Accessory Fuel Moisture (AFM) system. Although the AFM system was designed to supplement and support the needs of the other three subsystems, this system has not yet been developed in New Zealand (Figure 1). The intention of the AFM is to provide a method for estimating FMC for different fuels [29], at different times of the day [30] to supplement FWI moisture codes, providing data to the FBP and FOP components, as well as the NZFDRS (Figure 1). A near-real-time LFMC system can be converted into the AFM subsystem, providing both the FBP and FOP subsystems with fuel moisture data. This provides a direct pathway for the incorporation of a near-real-time LFMC system. The development of the AFM using an LFMC system will improve not only the fire danger ratings but may also improve the associated fuel moisture indices within the FWI system (e.g., drought code or fine fuel moisture code). The specifics of how the LFMC system can be integrated into the NZFDRS system are provided in Section 6.

Satellite remote sensing can be used to monitor LFMC in near-real-time across large areas and to provide timely updates on fuel type to aid interpretation. While scientists have been using satellite remote sensing to evaluate fuel characteristics since the 1980s, rapid improvements in satellite technology combined with increased data cadence provide new opportunities [10,31].

The robust interpretation of LFMC requires up-to-date knowledge of fuel type as ignition likelihood and fire behavior (rate of spread and intensity) varies for a given LFMC across different fuel types. Different fuel types have different fuel moisture thresholds for when combustion can be sustained, and wildfires can develop (e.g., moisture of extinction). Fuel types are vegetation classes sharing similar ignition likelihood and fire behavior. Various classification schemes for fuel types have been developed to suit different regional contexts. The vegetative cover types that make up fuel types have been predicted using remotely sensed data, which most often use multispectral reflectance to spatially segregate fuel cover types and Light Detection and Ranging (LiDAR) to provide detailed information on structural characteristics of the fuel type [32,33]. However, remote sensing of fuel moisture has most often been undertaken without up-to-date spatial characterization of the fuel type.

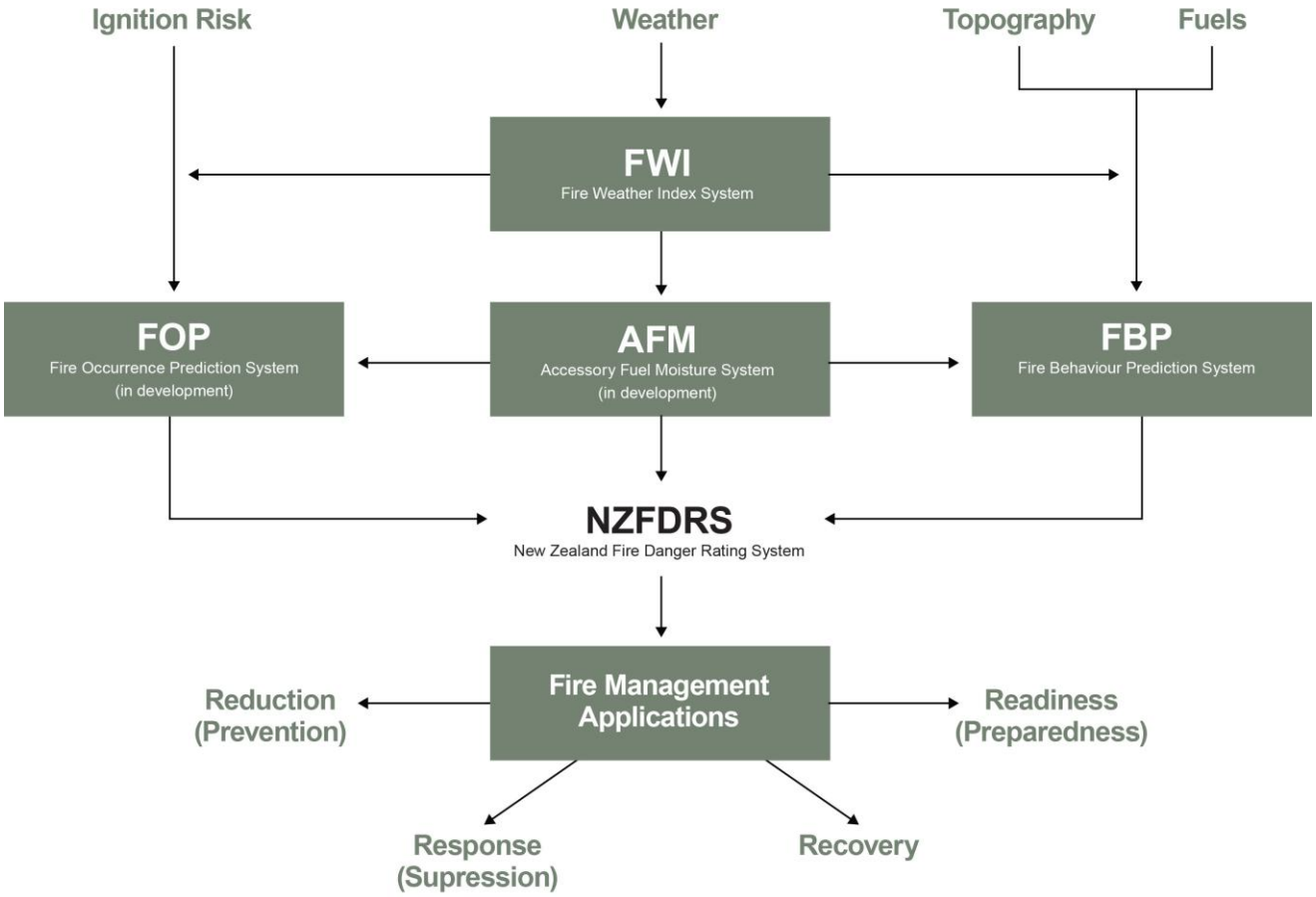


Figure 1. Structure of the New Zealand Fire Danger Rating System (NZFDRS). This is an updated image based on Anderson [28].

Recognizing these gaps, the aim of this review is to develop a roadmap for a near-real-time LFMC monitoring system using remote sensing, designed for direct integration into fire danger rating systems, using New Zealand as a case study. Establishing such a system will also expand global fuel moisture datasets by providing contributions from a region characterized by pronounced topographic heterogeneity, diverse vegetation types, and persistent cloud cover.

First, we review existing passive and active remote sensing technologies that have the capability to measure LFMC and map fuel types. We then examine modeling techniques for LFMC estimation and fuel type classification. Finally, we present an overview of how LFMC and fuel type can be integrated into fire assessments, at a broad international level and within a detailed New Zealand specific context. Building on these components, we present a pathway for implementation that includes how a near-real-time LFMC and a fuel type system for New Zealand can be integrated into fire behavior simulation tools, operational fire danger rating systems, and the forecasting of wildfire and drought conditions. Finally, we discuss key challenges and future directions and conclude with the expected benefits of this system for wildfire and drought management in New Zealand.

2. Review of Current Technology for LFMC and Fuel Type Monitoring

2.1. Available Satellite Instruments

Selecting an appropriate satellite instrument for monitoring LFMC and fuel types requires careful consideration of multiple interrelated factors. These include the type of sensor, its spectral, spatial, and temporal resolution, as well as the associated data processing requirements and limitations. There is considerable variation not only between

different sensor modalities (e.g., optical, thermal, radar) but also within each category, reflecting trade-offs in spatial and temporal resolution as well as regional/global satellite coverage (Figure 2). These attributes must be carefully aligned with the characteristics of the target variable to ensure that the selected satellite products are fit for purpose. Additionally, practical considerations such as data latency, availability (e.g., commercial vs. free access), and the ease of integration with other datasets also play a critical role in designing an effective satellite-based monitoring program.

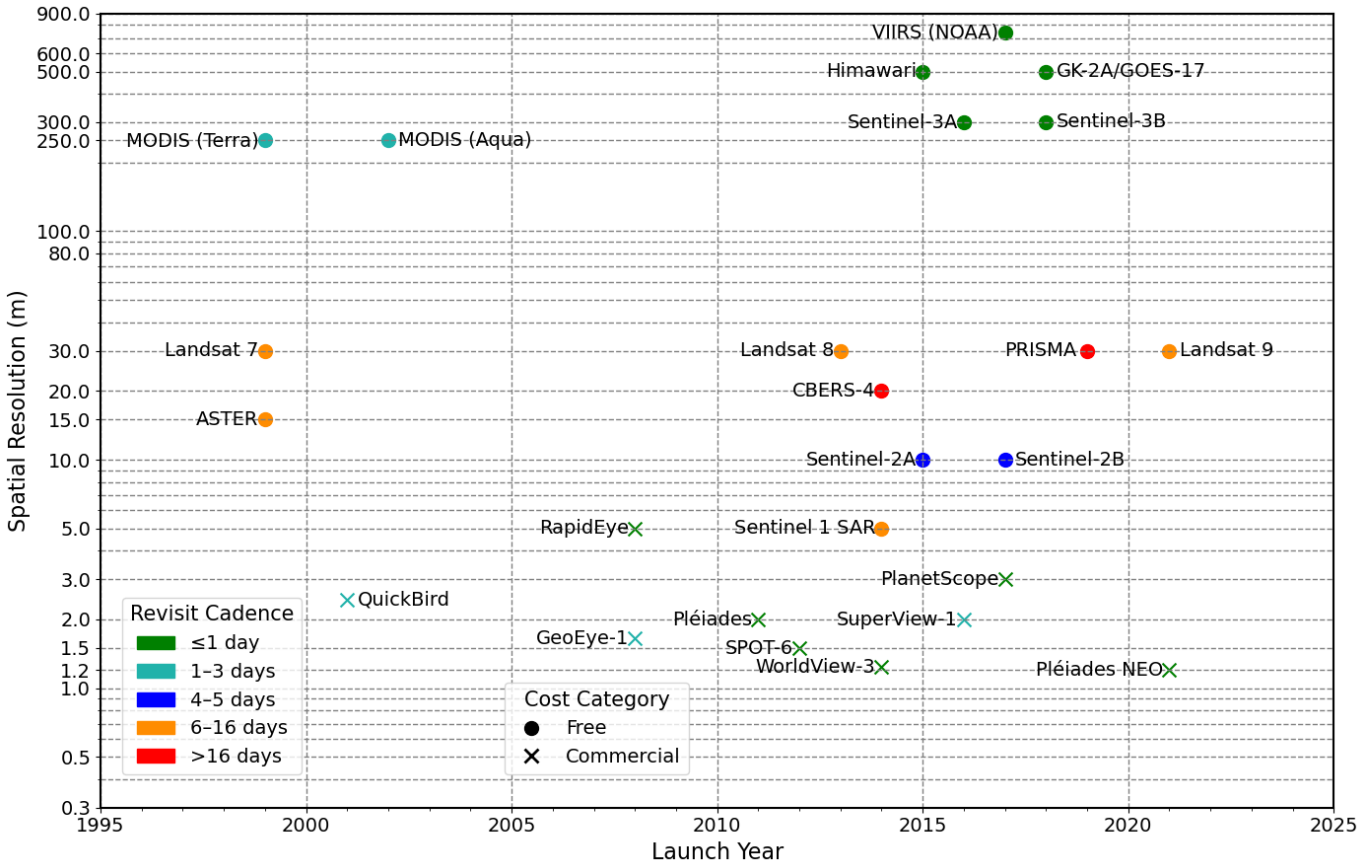


Figure 2. Variation in spatial resolution, revisit cadence and cost of selected satellites launched over the last 30 years. Spatial resolution is displayed using a logarithmic scale and is often given at the ground sampling distance (GSD) of the most fine-resolution spectral band. The revisit cadence for joint satellite constellations (e.g., Sentinel-2A and 2B) refers to the combined revisit interval achieved when both satellites operate together.

2.1.1. Overview of Sensor Types

Passive optical sensors measure sunlight reflected from the Earth's surface across visible (VIS), near-infrared (NIR), and shortwave infrared (SWIR) wavelengths [34]. While widely used due to their rich spectral information, these sensors have notable limitations. Their effectiveness is constrained by dependence on daylight and clear-sky conditions. Cloud cover, smoke, or dense vegetation canopies can obscure the surface signal, and no data can be acquired at night [35]. As a result, frequent observations or the use of gap-filling techniques is often necessary to compensate for missing data caused by atmospheric interference [35].

Thermal infrared (TIR) sensors detect emitted radiation (heat) from the Earth's surface, rather than reflected sunlight. Canopy surface temperature is a key variable measured by these sensors and has frequently been linked to plant water stress induced by drought [36–38]. Under drought conditions, reductions in stomatal conductance limit tran-

spiration, reducing evaporative cooling, resulting in higher canopy temperatures [39]. Many satellites host TIR sensors including [40]: Landsat (Thermal Infrared Sensor, TIRS/ETM+), Terra/Aqua (Moderate Resolution Imaging Spectroradiometer, MODIS), and Himawari-8/9 (Advanced Himawari Imager, AHI), enabling continental-scale monitoring of surface temperature. However, thermal sensors typically have coarser spatial resolution than their optical counterparts (Figure 2) and, like passive optical sensors, they are affected by cloud cover, as clouds absorb or obscure the emitted thermal radiation [41].

In contrast, active microwave sensors, such as Synthetic Aperture Radar (SAR) instruments aboard satellites like Sentinel-1, emit their own microwave pulses and measure the strength and timing of the backscattered signal from the Earth's surface. Unlike passive sensors, SAR does not rely on sunlight and can operate both day and night, regardless of weather conditions. The ability of SAR to penetrate cloud cover makes it particularly valuable for consistent monitoring in regions with frequent cloudiness. SAR signals can also partially penetrate vegetation canopies, depending on the wavelength and vegetation density, and are especially sensitive to surface characteristics such as soil moisture, vegetation structure, and surface roughness. The backscatter response varies with factors such as canopy water content, biomass, and underlying terrain. While SAR data offer unique advantages for observing surface and vegetation dynamics under a greater range of weather than passive sensors, interpreting these signals can be complex, as they are influenced by multiple interacting variables including canopy geometry, viewing angle, and surface wetness. Nonetheless, SAR provides a useful complementary data source to optical and thermal sensors in multi-sensor remote sensing frameworks [42,43].

Light Detection and Ranging (LiDAR) is another active remote sensing modality that uses laser pulses to measure the distance between the sensor and the target. By recording the time it takes for emitted pulses to reflect back from various surfaces, such as the ground, vegetation, and canopy layer, LiDAR can generate highly accurate three-dimensional structural information. Spaceborne LiDAR systems such as NASA's Global Ecosystem Dynamics Investigation (GEDI) provide valuable structural metrics (e.g., canopy height, vertical profile, foliage density) that are essential for estimating fuel loads and classifying fuel types. However, their sampling strategy, which involves acquiring data in discrete footprints along orbital transects, limits spatial continuity, and the low revisit frequency constrains temporal monitoring. Although airborne laser scanning (ALS) offers wall-to-wall coverage, it remains cost-prohibitive for large areas. Consequently, LiDAR is typically used as ancillary data to calibrate or validate models based on more spatially continuous datasets such as optical or SAR imagery [44–47].

2.1.2. Sensor Orbit Types and Revisit Cadence

Satellite orbit type has a fundamental impact on data frequency and consistency. Geostationary satellites remain fixed relative to the Earth's rotation, continuously observing the same region. Their key advantage is sub-hourly cadence. For example, the Himawari-8 geostationary satellite provides imagery every 10 min. However, geostationary platforms typically have coarse spatial resolution (Figure 2). Their fixed position leads to nearly constant viewing geometry for each ground location, which reduces angular variability across acquisitions but results in systematically large off-nadir angles away from the sub-satellite point. This can exacerbate geometric distortions and atmospheric path-length effects, adding variability to the data, particularly for high-latitude regions [48,49].

In addition to geostationary platforms, there are commercial high-resolution satellite constellations capable of providing daily or near-daily imagery. Notably, systems such as PlanetScope and Maxar's WorldView or Pleiades Neo series achieve frequent revisits (Figure 2) by deploying large numbers of small satellites in coordinated sun-synchronous

polar orbits, rather than through geostationary positioning. These constellations can image the same location each day, or even multiple times per day, by staggering satellite passes. While these systems offer exceptional temporal frequency (and spatial detail), they are commercial in nature, often requiring paid access and sophisticated infrastructure to manage large data volumes.

In contrast to commercial constellations designed for high revisit rates through large fleets, most publicly funded polar-orbiting missions rely on one or two platforms, resulting in longer revisit intervals. For example, Landsat 8 and 9 each have a 16-day repeat cycle, but together provide an effective combined revisit time of ca. eight days (Figure 2). Similarly, the twin Sentinel-2 satellites deliver a combined revisit cycle of ca. five days.

2.1.3. Spatial Resolution

Spatial resolution refers to the smallest object a sensor can detect [50] while the ground sampling distance (GSD) is the distance between the centres of two adjacent pixels [51]. The GSD fundamentally impacts the level of detail that can be observed. Very high-resolution (VHR; 0.5–5 m) commercial optical imagery comes from constellations such as Planet's PlanetScope (Dove/SuperDove satellites), Maxar's WorldView series (e.g., WorldView-2/-3), and Airbus's Pléiades Neo (Neo-3/-4). These systems capture very fine spatial detail and achieve frequent revisits through constellation size and agile off-nadir tasking but are costly and generate large data volumes, as many images are required to cover a region. As a result, high resolution data are often used in targeted analyses rather than continuous nationwide monitoring.

Moderate-resolution satellites, such as Sentinel-2 (10–20 m), Landsat-8 and -9 (30 m) offer a practical balance between spatial detail and coverage enabling reliable observation of landscape-scale patterns. Their resolution is typically sufficient to resolve dominant vegetation structures and land cover contrasts, while the high cadence of Sentinel-2 allows for updated observations every few days. Such sensors are well-suited to operational monitoring across broad areas with manageable storage and processing demands.

In contrast, coarse-resolution satellites such as MODIS (250–500 m), Visible Infrared Imaging Radiometer Suite (VIIRS; 750 m), and geostationary platforms like Himawari-8 and Geostationary Operational Environmental Satellite (GOES; typically 0.5–2 km) trade spatial precision for high temporal coverage. These systems are capable of daily or sub-daily observation, making them ideal for capturing rapid changes over large regions. However, their relatively coarser GSD limits their ability to resolve fine-scale spatial variability. As a result, their output often represents averaged signals across heterogeneous land covers, reducing their suitability for localized mapping tasks. Nonetheless, their consistency, frequency, and near-global coverage ensure they remain a valuable part of the Earth observation landscape, particularly for applications requiring broad-scale temporal continuity.

2.1.4. Spectral Resolution

Optical instruments vary in their spectral resolution, which refers primarily to the width of the wavelength bands they can distinguish, though practical differences also arise from the number and position of these bands across the electromagnetic spectrum. Multispectral sensors typically capture a limited set of broad, non-contiguous bands. The number of bands typically ranges from 4 to 15, with these bands covering selected portions of the visible (VIS; 400–700 nm) and near-infrared (NIR; 700–1100 nm) regions, and in some cases extending into the shortwave infrared (SWIR; 1100–2500 nm). The inclusion of SWIR bands is particularly important for detecting moisture-related properties, such as leaf water content. However, not all multispectral instruments include SWIR bands. For example, early-generation sensors or lower-cost systems may be limited to the visible

and NIR regions only. The specific spectral configuration varies by sensor: for instance, Sentinel-2 includes several bands in the red edge and SWIR ranges, whereas others such as PlanetScope focus on fewer broad bands primarily in the visible and NIR ranges.

In contrast, hyperspectral sensors measure reflectance in dozens to hundreds of very narrow, contiguous wavelength bands, typically spanning the visible to SWIR region (400–2500 nm). This continuous spectral coverage provides a near-complete reflectance curve for each pixel, enabling the detection of subtle biochemical features, such as specific water absorption bands, photosynthetic pigments, or dry matter content. Hyperspectral sensors, while offering greater spectral fidelity, are less frequently used for LFMC monitoring because of their limited availability, complex processing requirements, and generally low revisit frequency.

2.2. Estimation of LFMC

2.2.1. Physical Basis for Detection of LFMC

Effective prediction of LFMC using spectral satellite data relies on a robust set of bands that can detect water. Water exhibits strong absorption in NIR and SWIR wavelengths and previous research has found liquid water absorption peaks of increasing size at 970, 1200, 1450, 1950 and 2500 nm [52–57]. Consequently, common spectral indices for vegetation water content often use a SWIR or NIR band to detect water content and a NIR band to normalize the effect of leaf structural variability on reflectance (Table 1) [57,58]. Greenness indices based on visible and near-infrared (VNIR) bands have also shown significant empirical relationships with seasonal changes in LFMC across shrublands and forests, supporting their use as proxies for LFMC when SWIR data are unavailable [59,60]. Remote sensing using thermal bands can also be used to detect vegetation water status. As plants experience moisture stress, stomatal closure reduces transpiration, causing an increase in sensible heat and elevating canopy surface temperature [39]. This thermodynamic response has been widely exploited using thermal infrared remote sensing.

Microwave remote sensing also offers potential for assessing vegetation water content. Both active (e.g., SAR) and passive microwave sensors are sensitive to changes in the dielectric constant of biomass, which increases with higher water content in plant tissues. Wet leaves, stems, and branches exhibit stronger backscatter returns due to these dielectric properties [61]. For active microwave systems, this means that wet biomass generally produces a stronger and more variable backscatter return than dry biomass [62]. However, retrieving plant water content from microwave measurements is more complex than with optical/thermal methods, because the signal is influenced by many confounding factors. Variations in total vegetation biomass and structure, surface roughness, sensor viewing geometry, and terrain can all affect the microwave backscatter independent of water content [63]. Similar complexities have also been shown for passive microwave vegetation optical depth, which exhibits frequency-dependent and non-monotonic sensitivities to leaf area index and above-ground biomass [64].

Table 1. Selected studies using remotely sensed data to estimate live fuel moisture content (LFMC). Shown for each study are the year of the study, methods, sensors, indices, ancillary information, and the context of the study, including location and vegetation type. Also shown is the coefficient of determination (R^2) for the final model predicting LFMC. Abbreviations for the Method are: Empirical, empirical models; ML, machine learning models; RTM, radiative transfer model (physical models). Ancillary information abbreviations are: ST: surface temperature; DOY, day of year; LCT, landcover type; DM, dry matter; LAI, leaf area index; Ccov, canopy cover; DC, drought code. Indices shown in bold had the strongest relationships with LFMC among those listed for each study. Studies are separated by dashed lines.

Year	Method	Sensor	Indices	Ancillary Inf.	Vegetation	Location	R^2	Reference
2004	Empirical	AVHRR	NDVI	ST, DOY, LCT	Mediterranean grasslands	Spain	0.88–0.91	[65]
		AVHRR	NDVI	ST, DOY, LCT	Mediterranean shrubland	Spain	0.72	
2005	Empirical	MODIS	NDWI, **VARI**	None	Chaparral	California, USA	0.79–0.94	[26]
2005	Empirical	MODIS	NDVI, **NDWI**	None	Chaparral and coastal shrubland	California, USA	0.39–0.80	[66]
2007	RTM	MODIS		None	Pine stands; hardwood dominated areas	Georgia, USA	0.57–0.65	[67]
2008	Empirical	MODIS	NDVI, EVI, **VARI**, VIgreen, NDII6, NDII7, NDWI	None	Chaparral and coastal sage scrub	California, USA	0.85	[59]
2008	RTM	MODIS		LAI	Mediterranean grassland	Spain	0.927	[68]
	RTM	MODIS		DM	Mediterranean shrubland	Spain	0.703	
	Empirical	MODIS	**NDVI**, SAVI, EVI, GEMI, VARI, NDII6, NDWI, GVMI	None	Mediterranean grassland	Spain	0.914	
	Empirical	MODIS	NDVI, SAVI, EVI, GEMI, **VARI**, NDII6, NDWI, **GVMI**	None	Mediterranean shrubland	Spain	0.723	
2008	Empirical	AVHRR	NDVI	ST, DOY	Mediterranean grassland	Spain	0.83	[60]
		AVHRR	NDVI	ST, DOY	Mediterranean shrubland	Spain	0.71	
2011	Empirical	MODIS	NDIImax − min, VARImax − min	None	Shrubland, heathland, sclerophyll forest	SE Australia	0.69	[69]
2012	Empirical	AISA Eagle Hawk	Reflectance, first derivatives, **MSI**, WI, NDWI, TM5/TM7, NDVI, NDII	None	*Calluna vulgaris* and grassland	Central Pennine uplands, UK	0.75	[70]
2013	RTM	MODIS		LAI, Ccov	Woodlands	Spain	0.50	[25]
2018	Empirical	AMSR-E	microwave data	None	Forests, shrublands, grasslands	Mediterranean	0.32	[71]
	Empirical	MODIS	**VARI,** SAVI, NDVI, NDWI, NDII6, NDII7, GCMI	None	Forests, shrublands, grasslands	Mediterranean	0.44	
2018	Empirical	MODIS	**NDVI**, NDII6, NDII7, GVMI, NDWI, EVI, SAVI, **VARI**, VIgreen	None	Mediterranean shrubland	Spain	0.85	[72]
	Empirical	Sentinel-2	**NDVI**, NDII6, NDII7, EVI, SAVI, **VARI**, VIgreen	None	Mediterranean shrubland	Spain	0.76	
2018	Empirical	MODIS	EVI	Tmin	Chaparral, shrubland	California, USA	0.68–0.73	[73]
2020	Empirical	Landsat-5 TM	NDVI, NDII, **EVI**, VARI	Terrain	Chaparral	western USA	0.48	[15]
2020	Empirical	MODIS	**VARI, Vigreen, GVMI, NDWI, NDVI**	None	Mediterranean shrubland	Spain	0.69–0.78	[74]
	RTM	MODIS		None	Mediterranean shrubland	Spain	0.49	
2020	ML	Sentinel-1		Soil, LiDAR ht, elevation, slope, NDVI, NDWI, LCT	All	western USA	0.63	[43]
	ML	Sentinel-1			Shrub/grassland	western USA	0.56	
	ML	Sentinel-1			Grassland	western USA	0.56	
	ML	Sentinel-1			Mixed forest	western USA	0.59	
	ML	Sentinel-1			Closed needleleaf evergreen	western USA	0.61	
	ML	Sentinel-1			Closed broadleaf deciduous	western USA	0.49	
	ML	Sentinel-1			Shrubland	western USA	0.69	
2020	RTM	Himawari-8		None	croplands, trees	Australia	0.26	[48]
	RTM	MODIS		None	croplands, trees	Australia	0.67	
2021	Empirical	Sentinel-2	EVI, SAVI, OSAVI, NDVI, RVI, VARI, **NDMI**, NDWI, VIgreen, TCARI, TCARI/OSAVI, SLA	Met. data	Mediterranean shrubland	Eastern Spain	0.70	[75]

Table 1. *Cont.*

Year	Method	Sensor	Indices	Ancillary Inf.	Vegetation	Location	R^2	Reference
2021	ML	MODIS	Band reflectances	Elevation, slope,	Cropland	Contiguous USA	0.64	[76]
	ML	MODIS	Band reflectances	aspect, latitude,	Grassland	Contiguous USA	0.58	
	ML	MODIS	Band reflectances	longitude,	Forest	Contiguous USA	0.42	
	ML	MODIS	Band reflectances	DOY	Shrubland	Contiguous USA	0.67	
2022	ML	MODIS	Band reflectances	Climate data, climate zone, topography, location, DOY	All vegetation classes	Contiguous USA	0.70	[77]
2022	ML	Sentinel-2	**VARI**, ARVI, RVI2, TCARI/OSAVI, NMDI	Elevation, Slope, north, east, Ht	Oaks, pines, shrubland, grassland	Spain	0.55	[78]
	ML	Sent-2/ancill.	**VARI**, ARVI, RVI2, TCARI/OSAVI, NMDI		Oaks, pines, shrubland, grassland	Spain	0.63	
	ML	Sentinel-1 SAR			Oaks, pines, shrubland, grassland	Spain	0.28	
2022	ML	Sentinel-1 (S1)	NDWI, NDVI, NIRV, 5 band reflectances 7 Band reflectances	Soil, LiDAR ht, LCT, elevation, slope	Forests, shrublands, grasslands	western USA	0.53	[42]
	ML	Landsat-8 (L)			Forests, shrublands, grasslands	western USA	0.7	
	ML	MODIS (M)			Forests, shrublands, grasslands	western USA	0.74	
	ML	L+S1			Forests, shrublands, grasslands	western USA	0.81	
	ML	M+S1			Forests, shrublands, grasslands	western USA	0.81	
	ML	M+L+S1			Forests, shrublands, grasslands	western USA	0.85	
2023	Empirical	Sentinel-2	EVI, OSAVI, **TCARI**, Vgreen, VARI, **MSI**, NMDI	rainfall, slope	Mediterranean shrubland and trees	Eastern Spain	0.74	[79]
2024	RTM	Himawari		None	Grassland, evergreen forest	Australia, China	0.60–0.61	[49]
	RTM	Landsat-8 OLI		None	Grassland, evergreen forest	Australia, China	0.68–0.79	
	RTM	MODIS		None	Grassland, evergreen forest	Australia, China	0.63–0.76	
2025	ML	MODIS	NDVI, NDWI, NDII6, NDII7, **GVMI**, EVI, SAVI, VARI, VIgreen, **NDTI**, STI, MSI, Gratio	DC, DOY	Shrubland	Portugal	0.78	[80]

2.2.2. Predictions of LFMC Within the Literature

A wide range of satellite sensors have been used for LFMC prediction, spanning optical, thermal, and microwave domains. Details of selected studies conducted over the last 21 years are presented in Table 1. The chronological arrangement of studies in Table 1 highlights the evolution of LFMC estimation approaches, from early empirical analyses using coarse-resolution sensors (e.g., AVHRR, MODIS) to more recent applications of machine learning incorporating higher-resolution sensors such as Sentinel-2. This list builds on a previous review by Yebra et al., 2013 [11] focusing on studies that reported model performance using the coefficient of determination (R^2) as this widely used statistic allowed a broad number of comparisons.

Publicly funded multispectral sensors, with NIR and SWIR bands dominate LFMC research due to their balance of spectral resolution, accessibility and ease of processing. Among optical sensors, MODIS has been the most widely used globally (Table 1), owing to its near-daily global coverage from both morning and afternoon overpasses, and excellent spectral coverage with SWIR bands at 1.24, 1.64, and 2.13 µm [40].

Although not as widely used as MODIS over the last two decades, the number of studies using Sentinel-2 and the Landsat series sensors has increased markedly over the last 5 years. This temporal trend is evident in Table 1, where studies published after 2018 increasingly use Sentinel-2, reflecting the growing accessibility and reliability of this sensor for operational LFMC monitoring. Sentinel-2A and 2B (MSI) provide 13 spectral bands, including two SWIR bands (1.61 and 2.19 µm) and several red-edge bands that enable refined vegetation monitoring. These satellites are becoming more widely used due to their higher spatial resolution and consistent global availability [15,72,75,79]. The Harmonized Landsat Sentinel (HLS) dataset enhances this coverage by integrating data from both Landsat and Sentinel-2 into a single, radiometrically consistent product. HLS includes the requisite NIR and SWIR bands for LFMC estimation (Figure 3), has a GSD of 30 m, and can be supplied at a 2–3 day cadence, with a latency of 1.7 days.

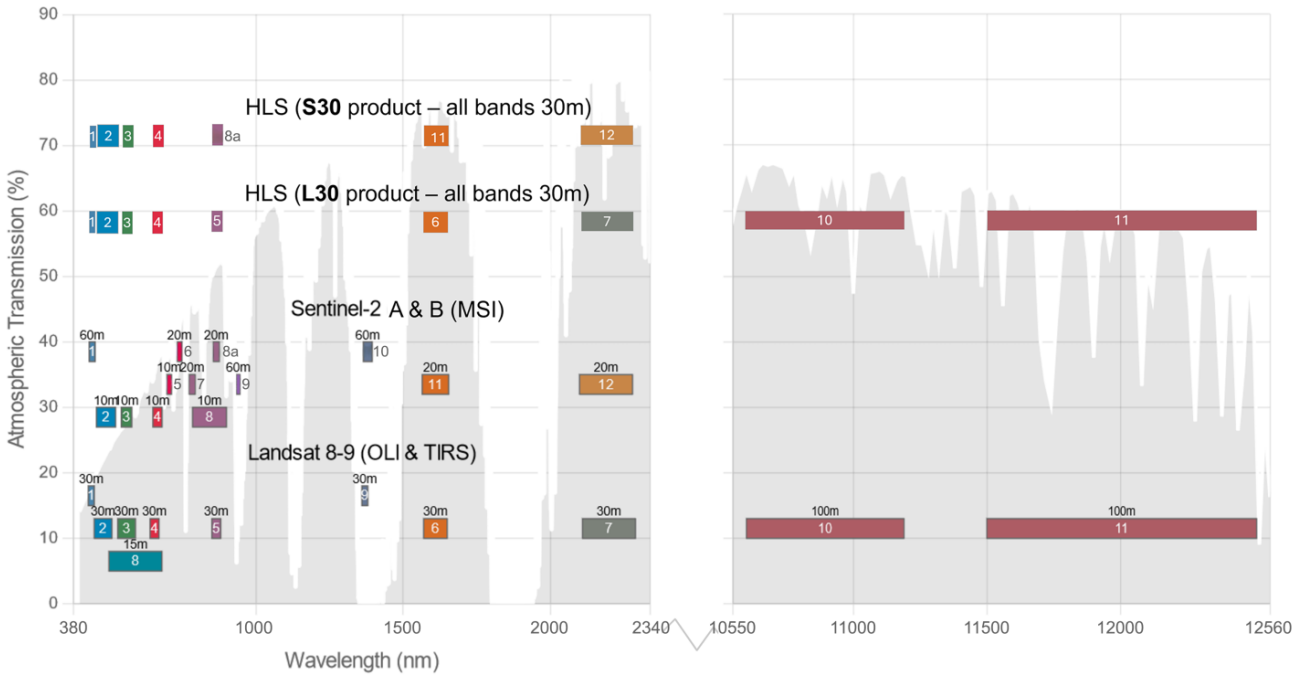


Figure 3. Structural band comparison for the Harmonized Landsat Sentinel product (HLS) showing the bands for the Sentinel-2 (S30) and Landsat (L30) products. Also shown are the bands for Sentinel-2 and Landsat 8–9 data from which HLS is derived. The different numbers and colors in the figure denote different bands within Sentinel 2 and Landsat 8–9.

In addition to widely used polar-orbiting platforms, geostationary satellites such as Himawari-8, which has high temporal resolution, have also been explored for LFMC prediction [48,49] (Table 1). Microwave remote sensing has been widely used for LFMC estimation (Table 1), and a very common platform is Sentinel-1 [42,43,71,78,81]. Very high-resolution satellites have not been widely used for LFMC prediction as these often provide more detail than is operationally useful and processing this detailed data is computationally demanding.

Comparative studies between MODIS and Sentinel-2 data show little difference in predictive accuracy [72]. However, superior predictions from MODIS have also been reported which was attributed to a lower number of Sentinel-2 images from which to select [74]. This limitation may now be partly remedied with improved data cadence and the assembly of the HLS dataset. While MODIS has been a cornerstone of LFMC monitoring to date, it is approaching the end of its operational life, and VIIRS has been identified as a successor. However, VIIRS has coarser spatial resolution than MODIS in critical spectral regions, including the NIR (375 m vs. 250 m) and SWIR bands (750 m vs. 500 m). In contrast, Sentinel-2 and HLS both provide sufficient spatial and spectral resolution to capture LFMC variability (Figure 3). Combined with open global access and the frequent revisit intervals possible with HLS, these attributes make them highly suitable for large-scale LFMC monitoring.

Combining SAR, which can penetrate cloud cover, with multispectral data offers distinct advantages for LFMC prediction. Sentinel-1 C-band SAR has been widely explored for this purpose due to its free availability, high spatial resolution, and relatively short revisit interval (six days over New Zealand). In comparative studies [42,78], predictions of LFMC using only satellite microwave data are generally less accurate than use of only optical data (Table 1). However, studies also show that microwave data provides a valuable complement to optical data [71,81] and incorporating SAR with multispectral inputs has been shown to improve predictions of LFMC (Table 1) [42,43], although contrasting results have also been reported [78]. Overall, these findings underscore the potential for developing an operational LFMC prediction system that leverages both the HLS product and Sentinel-1 SAR data. This approach is especially valuable in persistently cloudy regions such as New Zealand.

Ancillary information has been widely used in models of LFMC and can significantly improve the accuracy of predictions (Table 1). Typically used information includes day of the year, landcover type, dry matter, leaf area index, canopy cover and canopy height. Meteorological data has also been widely used for both current predictions (Table 1) and to forecast LFMC up to three months in advance [82].

Meteorological variables used in models of LFMC have most often been derived from gridded surfaces developed through interpolation of meteorological station data [75,77]. These datasets, which can have spatial resolutions as fine as 4 km, typically include variables such as precipitation, air temperature, rainfall, vapour pressure deficit (VPD), relative humidity and windspeed [75,77]. Several drought indices, including the Keetch-Byram Drought Index and the Cumulative Water Balance Index have also been derived from meteorological data and used to predict LFMC [83].

Although satellite-derived estimates of meteorological variables are available there has been limited use of this data source in LFMC models. Satellite derived estimates of VPD can be extracted from thermal and near-infrared observations measured by MODIS [84]. Soil moisture information can be sourced from satellite remote-sensing platforms, such as the European Space Agency's Soil Moisture Ocean Salinity (SMOS) mission which uses L-band radar to estimate volumetric soil moisture in the upper ~5 cm of soil at a spatial resolution of 43 km [85]. Although SMOS and other satellite derived soil-moisture products

show good agreement with in-situ measurements [86,87] and have demonstrated utility in prediction of the McArthur Forest Fire Danger Index [88] their direct use in LFMC modelling remains limited.

2.3. Predictions of Fuel Type

2.3.1. Fuel Type Classification

Fuel types are groupings of vegetation with similar physical properties that determine how they behave during combustion. More precisely, a fuel type is defined as "an identifiable association of fuel elements of distinctive species, form, size arrangement, and continuity that will exhibit characteristic fire behavior under defined burning conditions" [89]. These groupings enable simplification of complex vegetation fuel environments for fire behavior prediction, planning, and management.

A wide range of vegetation characteristics have been used to define fuel types. In addition to vegetation type and species, structural attributes include vegetation cover, canopy bulk density, crown base height, apparent crown density, biomass, stand density, vertical continuity, and spatial arrangement of fuel layers. Other critical properties relevant to wildfire risk include live and dead fuel loads and their moisture content [90,91]. Because it is impractical to characterize all physical traits in situ, classification systems typically group vegetation into fuel types that approximate fire behavior under standardized conditions.

Numerous fuel classification systems have been developed to support different fire modeling frameworks around the world. These systems vary in complexity, purpose, and regional applicability. The Canadian Fire Behavior Prediction (FBP) System, for instance, distinguishes 16 discrete fuel types grouped into five major categories: coniferous, deciduous, mixed-wood, slash, and open (grass) fuels. Each type is qualitatively described by forest composition, stand structure, and surface fuel conditions, with examples such as mature or immature jack/lodgepole pine [92,93]. In contrast, the Prometheus classification developed for Mediterranean Europe categorizes fuels into seven types, grouped by dominant propagation elements (grass, shrubs, or ground litter) using variables such as fuel height and horizontal continuity [94].

Despite their utility, fuel type classifications have limitations. First, fuel models are inherently site-specific and systems developed for one geographic or ecological setting may not perform well elsewhere (e.g., [95]). Second, structural fuel characteristics—which are often more critical than species identity, especially during drought/dry conditions for predicting fire behavior—can be difficult to quantify without intensive field data or remote sensing. Third, most fuel maps represent static conditions, yet fuel properties evolve over time due to growth, succession, disturbances, or management interventions. However, the maintenance of up-to-date fuel type maps is both resource-intensive and methodologically challenging using traditional mapping approaches such as field surveys or aerial photo interpretation [32,33]. Ideally, fuel type classifications should be updated at least annually.

2.3.2. Use of Remote Sensing to Classify Fuel Types

The potential of remote sensing to classify and regularly update fuel types has been well established and has been the focus of two significant reviews [32,33]. The more recent review [33], which examined studies conducted between 2008 and 2022, found that moderate-resolution multispectral satellite sensors were the most frequently used data source for fuel type classification, and used in 37% of the reviewed studies. These included platforms such as Landsat-8 and Sentinel-2, which offer broad coverage, key spectral bands for vegetation analysis, and free accessibility. Hyperspectral sensors, mounted primarily on airborne platforms (e.g., Airborne Visible/Infrared Imaging Spectrometer (AVIRIS), Multispectral Infrared and Visible Imaging Spectrometer (MIVIS)), were used in 32% of

the studies and provided high spectral fidelity for differentiating fuel types with similar spectral signatures. VHR multispectral satellite data (e.g., WorldView, QuickBird) were employed in 21% of cases, while airborne laser scanning was used in 10% of studies. The earlier review [32] emphasized the value of SAR for fuel type mapping, citing its demonstrated ability to capture structural forest attributes relevant to fire behavior, such as canopy closure, foliar biomass, tree height, and volume [96].

Reported overall classification accuracies (OA) for fuel type mapping vary widely between studies, sensors, and modelling approaches, ranging from 50% to 95% [32,33]. While direct comparisons between sensors across this literature are hindered by the diversity of classified fuel types and methodological differences, some studies using the same datasets provide useful insights. In a study that mapped the seven Mediterranean fuel types, the use of Hyperion hyperspectral imagery with a 30 m resolution produced a classification virtually identical to that of Landsat TM multispectral imagery (OA = 70%). However, VHR QuickBird imagery (2.4 m resolution) outperformed both (OA = 74.7%), suggesting that spatial resolution may be more influential than spectral resolution [97]. This was consistent with Roberts et al., 2003 [98] who observed significantly higher classification accuracy using high-resolution airborne hyperspectral data from AVIRIS compared to lower-resolution satellite derived hyperspectral data from the Hyperion sensor (OA = 79% vs. 50%)

Numerous studies have demonstrated that combining data from multiple sensors improves classification accuracy. In comparative studies, the addition of ALS to satellite multispectral data has consistently been found to improve the accuracy of predictions [44–47]. For instance, the addition of LiDAR data to Quickbird satellite imagery provided an overall classification accuracy of 90% for grasses, shrubs and forest fuel types in East Texas, which was a 14% improvement on use of only Quickbird imagery [99]. Similarly, combining ALS with airborne hyperspectral data has yielded higher accuracies than use of hyperspectral data alone for classification of forest, savanna and shrubland in Hawaii [100]. Satellite SAR data remains an attractive option as a supplementary input, especially when combined with spectral datasets, due to its cost-effectiveness and global availability [101].

Topographic variables derived from LiDAR-based digital terrain models have also been found to enhance fuel type classification. Given that fuel types are often influenced by elevation, slope, and aspect, incorporating these predictors into models has consistently improved classification performance. Significant gains in accuracy have been reported when topographic variables were combined with satellite multispectral imagery [102] and Sentinel-1 SAR data [101].

3. Modelling Methods for Predicting LFMC

The estimation of LFMC using satellite data has involved several modelling approaches, each with its unique methodology, strengths, and limitations. These approaches can be broadly categorized into empirical parametric models, machine learning approaches, and physical models such as Radiative Transfer Models (RTMs) [11,77]. The choice of modelling approach depends on various factors, including data availability, computational resources, and the specific requirements of the application. This section delves into these modelling approaches, providing an overview of their methodologies and highlighting their respective strengths and weaknesses.

3.1. Empirical Models

Empirical models estimate LFMC by fitting statistical relationships between ground measurements and satellite-derived reflectance and spectral indices [11]. They are typically parametric and include linear regression, multivariate linear regression (MLR), non-linear regression (NLR), and generalized additive models (GAMs). While linear regression offers

a straightforward approach, MLR, NLR, and GAMs provide greater flexibility and can perform better in complex or heterogeneous environments. In studies that select indices from a group, the Visible Atmospherically Resistant Index (VARI) was the index most widely used to predict LFMC, followed by the Normalized Difference Vegetation Index (NDVI), then the Global Vegetation Moisture Index (GVMI) and Moisture Stress Index (MSI) (Table 1). As VARI is based on blue, red and green reflectance, it is readily derived from virtually all multispectral sensors, supporting broad deployment across platforms.

Empirical approaches are the most widely used for LFMC and commonly achieve moderate-to-high accuracy (R^2 range 0.32–0.94; Table 1). They are straightforward to implement and calibrate [65,68,103], and they perform well where spectral–LFMC relationships are stable within, for instance, ecosystems with relatively uniform vegetation or long-term calibration datasets. By leveraging observed correlations between remotely sensed predictors and field LFMC, these models deliver reliable, context-specific estimates without requiring detailed process knowledge [104]. They are computationally efficient which is an advantage in operational wildfire settings that demand rapid processing during active incidents. Their simplicity enables use with standard statistical software and modest infrastructure, facilitating scaling across regions and vegetation types when supported by suitable calibration data (e.g., [79]). Collectively, these attributes make empirical models a practical option for operations, as emphasized by Yebra et al., 2013 [11].

Transferability and data dependence are the principal limitations of empirical models. Performance often degrades outside the calibration domain, necessitating sensor- and site-specific recalibration [105]. Vegetation heterogeneity, particularly in open shrublands, can reduce model accuracy when applied beyond their original context, as relationships often weaken under different species assemblages or climates [106]. Strong site-level correlations may also diminish when data from multiple regions are pooled due to variation in species composition, environmental conditions, and sampling protocols, underscoring the need for careful local calibration, validation, and region-specific models [15].

Robust performance depends on high-quality, representative in situ LFMC data to establish and validate the spectral relationships. However, obtaining such data is labor-intensive, time-consuming, and challenging in remote or inaccessible areas. Open-access LFMC databases improve feasibility [23,72,74], yet many applications remain local in scope and require bespoke calibration [68,74,107]. Accuracy is also contingent on current land-cover maps to minimize background and structural confounding factors [105]. Finally, in dense, closed canopies, spectral indices can saturate, limiting sensitivity to LFMC variation and obscuring vertical moisture differences, which constrains the ability of empirical models to capture the full range of LFMC dynamics in such environments [15].

3.2. Machine Learning

Machine learning (ML) models have become increasingly popular for estimating LFMC because of their ability to capture complex and non-linear relationships in large datasets [76,82]. As shown in Table 1, the use of these methods for predicting LFMC has grown rapidly with ML being more frequently used than empirical models over the last five years. Random forest (RF) is one of the most frequently used approaches due to its simplicity, robustness, and ability to manage many covariates without predefined functional forms. As an ensemble learning method, RF integrates multiple decision trees to improve accuracy and stability in regression tasks. Deep learning (DL) models also show strong potential, leveraging multi-layer networks to extract complex features automatically from large datasets [82].

ML approaches are particularly valuable in ecological applications because they can represent non-linear interactions among vegetation, soil moisture, and climate, which are

often interdependent. RF and neural networks detect such patterns, while DL models can approximate complex non-linearities among diverse bio- and geophysical parameters [76]. These models are capable of integrating diverse datasets, that include spectral indices, canopy cover, topography, soil moisture, and meteorological variables, providing robust LFMC predictions across varied environments [42,78,82,108]. Adaptability is another strength, as ML models can incorporate new data types as they become available, improving predictions over time. Numerous studies have demonstrated their ability to predict LFMC with moderate-to-high accuracy (Table 1) in heterogeneous landscapes [42,76,104] and comparisons show ML can outperform empirical models [109]. This capacity to integrate diverse data streams and adapt to dynamic conditions gives ML models a clear advantage over empirical approaches.

Despite these strengths, ML models have notable limitations. Training typically requires large datasets and substantial computational resources, particularly for DL and ensemble methods, which need specialized hardware such as Graphics Processing Units (GPU) [76,82,104]. Real-time or near-real-time LFMC prediction increases these demands, requiring rapid processing and frequent updates. Interpretability is another challenge. ML models often operate as black boxes, with numerous parameters and interactions that are difficult to explain [42]. Overfitting is also a risk, especially with complex models, where noise is mistaken for underlying patterns, reducing performance on unseen data [78]. The mitigation of overfitting requires training with datasets that capture a wide range of vegetation types and climatic gradients. Techniques such as cross-validation, feature selection, and regularization help reduce bias and improve generalization [82,104,110]. While powerful, ML approaches demand careful implementation, high-quality training data, and strategies to manage computational costs, interpretability, and overfitting to ensure reliable LFMC estimation.

3.3. Physical Models

Radiative transfer models (RTMs) for LFMC estimation offer a detailed and comprehensive representation of the processes that govern vegetation moisture content. RTMs consider the optical properties of vegetation, simulating how changes in moisture content influence radiation absorption, scattering, and emission, leading to more physically consistent LFMC estimates. By identifying the simulated spectra that most closely match the observed data, the model assigns LFMC-related parameters, often enabling accurate retrieval of moisture estimates with a physical basis. For instance, RTM inversions, using MODIS data over Mediterranean grasslands and shrublands in Spain have predicted LFMC with a close correlation to field measurements (R^2 range of 0.732–0.907) [68]. Simulated spectra in this RTM were based on the leaf level PROSPECT coupled with the canopy level SAIL RTM. At a broader scale a physically based retrieval model was used to estimate FMC across Australian grasslands, shrubland and forest from MODIS data using radiative transfer model inversion. Spectral signatures were simulated by coupling PROSPECT with SAILH for the grassland and shrubland and with the canopy level RTM GeoSAIL to simulate the forest spectra. Using observations of LFMC at 32 locations across Australia, model predictions were reasonably robust (R^2 = 0.58; RMSE = 40%) and did not require site specific calibration [111].

Because they encode universal physical laws, RTMs provide physically consistent LFMC estimates and are relatively generalizable [11]. This generality supports applications across diverse ecosystems ranging from deserts to tropical forests [68], and allows transferability across different sensor configurations [112]. By explicitly coupling canopy/leaf optics to physiological traits and moisture state, RTMs can yield more transferable predictions than purely statistical approaches [48,49,113]. Incorporating ecological rules and biophysi-

cal constraints further improves realism and robustness across diverse environments [113]. This generality has been demonstrated by research that has developed daily predictions of FMC at a global scale using MODIS data and RTM inversion methods [113]. The RTM models PROSPECT-5 (leaf level) and 4SAIL (grass and shrub canopy level) and GeoSail (tree canopy level) were used to generate look up tables (LUT) for all three vegetation types. Using a total of 3,034 FMC measurements from 120 worldwide sites as a validation dataset, the predictions of FMC were statistically significant and relatively accurate, particularly after low quality field measurements were excluded (R^2 = 0.71, RMSE = 32.36%).

However, RTMs do have limitations. They are inherently complex and computationally demanding, due to their detailed simulation of physical processes [106]. Inverting RTMs by aligning observed spectral reflectance with simulated outputs is costly computationally, but effective mitigation strategies have been developed. For example, some researchers have developed ML models based on RTM LUT which is not as computationally expensive. The ill-posed inverse problem, which is common in RTMs, occurs when different input parameters produce similar reflectance values, resulting in uncertainties during inversion [11].

Effective application of RTMs depends on extensive parameterization and calibration (e.g., LAI, soil/background properties, canopy structure), along with high-quality inputs that are not always readily available. Assumptions about canopy architecture or homogeneity may be violated in complex landscapes, degrading predictive accuracy. Sensitivity to input errors means small discrepancies in reflectance, ancillary meteorological data, or structural parameters can propagate to large LFMC biases [49]. Consequently, careful model selection, well-designed constraints, and rigorous calibration/validation are essential; otherwise, the operational value of RTMs can be compromised relative to simpler empirical approaches.

4. Modelling Methods for Predicting Fuel Types

The accuracy of LFMC estimations from empirical and RTM models are contingent upon having accurate and updated land cover maps [105], because different vegetation types have unique moisture dynamics that significantly influence fire behavior. LFMC varies greatly across fuel types, directly impacting their ignition potential and fire spread. By accurately classifying these fuels, they can be used as an explanatory variable for LFMC estimation models. The integration of fuel type as an explanatory variable can account for the specific moisture retention and loss characteristics of each vegetation type. This integrated method enhances the accuracy and spatial detail of models, leading to better predictions of drought and fire behavior.

Fuel type classification models commonly utilize data from remote sensing platforms, such as satellites or aerial sensors, to classify the landscape into different fuel types. These classifications are often based on the unique spectral signatures of the vegetation present in the remote sensing image. Some of the most common fuel type classification approaches include pixel-based (PB) models, object-based image analysis (OBIA), spectral mixture analysis (SMA) and deep learning (DL), each with its unique methodology, strengths, and limitations. The choice of modelling approach depends on various factors, including data availability, computational resources, and the specific requirements of the application.

4.1. Pixel-Based Models

Pixel-based (PB) models for fuel type classification use algorithms to categorize each pixel in remote sensing imagery into distinct fuel types based on spectral, spatial, and contextual features. These models typically leverage ML and statistical methods to manage large datasets and complex feature relationships, enhancing both the accuracy and efficiency

of classification. PB methods provide fine-grained mapping of fuel types at the pixel level, improving the understanding of spatial variability. However, they often treat each pixel as an independent entity, overlooking spatial interactions with neighboring pixels. This limitation can lead to challenges with mixed pixels, where multiple fuel types are present within a single pixel, resulting in a "salt and pepper" effect that diminishes the clarity of classification results [33].

Despite limitations, PB models can effectively classify fuel types, especially when multi-source data are integrated. For instance, addition of topographic variables to spectral and backscatter data from Sentinel-1/-2 was found to markedly improve classification accuracy of fuel types in north-eastern Greece resulting in an OA of 92.76% [101]. Similarly, the combination of environmental variables, Sentinel-2 imagery and LiDAR data provided significant synergies in classifying cool temperate rainforests/mixed forests with an OA of 88% for a model with all three data sources [114]. Advanced ensemble schemes further strengthen PB performance: an adaptive-stacking framework on Google Earth Engine using Sentinel-1/-2 and a digital elevation model (DEM) data outperformed single classifiers (e.g., SVM, RF), reducing "salt-and-pepper" noise and sharpening class boundaries for a wetland [115].

4.2. Object-Based Image Analysis

Object-based image analysis (OBIA) supports fuel type classification by segmenting imagery into meaningful objects that group pixels with similar spectral, spatial, and textural characteristics. Unlike pixel-based methods that classify pixels independently, OBIA incorporates spatial context and structural patterns of vegetation, producing more coherent classifications and reducing the 'salt-and-pepper' effect common in PB outputs. Its advantages were evident in wetland mapping with high-resolution UAV imagery, where OBIA achieved markedly higher OA than PB classification (70.8 vs. 61.9%) [116]. By integrating multispectral imagery, LiDAR, DEMs, and contextual information, OBIA further enhances fuel maps, particularly in complex ecosystems where vegetation types share similar spectral signatures but differ in structure or spatial arrangement.

However, OBIA's segmentation process can be computationally intensive and requires careful calibration to avoid over- or under-segmentation, making it more complex than pixel-based methods. Additionally, for VHR images, OBIA may struggle to define objects meaningfully due to the small size of individual features. While OBIA reduces the "salt and pepper" effect, it can also lead to over-smoothing, where fine details or transitions between land cover types are lost, reducing precision in highly heterogeneous areas.

4.3. Spectral Mixture Analysis

Spectral Mixture Analysis (SMA) is a technique in remote sensing that decomposes a pixel's spectral signature into its constituent components, or endmembers, making it particularly valuable for fuel type classification. Unlike traditional methods that assume each pixel represents a single class, SMA accounts for mixed pixels, especially in heterogeneous landscapes, by identifying and quantifying the proportions of different endmembers, such as grasses, shrubs, trees, and bare soil. This sub-pixel analysis improves the accuracy of fuel mapping in complex ecosystems, enabling better identification of fire-prone areas. SMA is highly adaptable, as it can be applied to various remote sensing data types, and it excels in handling mixed pixels. However, its success relies on selecting appropriate endmembers, and the process can be computationally demanding, especially when using hyperspectral data with numerous bands. Additionally, SMA can encounter challenges with spectral confusion when different fuel types share similar signatures. It is also sensitive to noise, which can reduce the precision of its results.

Several studies have applied SMA for sub-pixel vegetation fractional cover. Degerickx et al. (2019) [117] adapted SMA to account for the lower spectral and spatial resolution of Sentinel-2 imagery compared to other sensors. By simplifying the analysis and merging land cover classes (e.g., combining shrubs and trees into a "high vegetation" class), the study improved classification accuracy with the aid of height fraction data derived from LiDAR. Malhi et al. (2024) [118] applied SMA with AVIRIS-NG hyperspectral data to map plant functional types in a heterogeneous forest. The resulting fractional abundance maps revealed detailed spatial distributions of plant functional types, offering deeper insights into vegetation composition compared to traditional classification methods. Accurate endmember selection based on field observations was critical to SMA's success, underscoring the value of careful selection of endmembers that allow for better representation of the mixed pixel compositions in the hyperspectral data.

4.4. Deep Learning

Deep learning (DL) has become a highly effective tool for vegetation type classification in remote sensing, offering significant improvements over traditional methods. By utilizing neural networks, particularly convolutional neural networks (CNNs), DL can automatically extract complex spatial and spectral features from remote sensing data, leading to more precise identification of fuel types in diverse and heterogeneous landscapes. DL models can integrate multiple data sources, such as satellite and aerial imagery, streamlining the process and reducing the need for manual feature engineering. This capability enables the production of more detailed fuel maps, which are essential for accurate fire risk assessment and effective ecosystem management.

However, DL also has its challenges. The method requires large amounts of labeled training data, which can be expensive and difficult to collect, particularly for diverse and complex ecosystems. The computational demands are high, often requiring significant processing power and time for model training. Furthermore, DL models are often viewed as "black boxes" due to their complexity, making it hard to interpret the decision-making process. There is also the risk of overfitting, especially when the training data does not fully represent the variability in fuel types, which can limit the ability of the model to generalize to new areas or conditions.

Recent comparisons of pixel-based (PB), object-based image analysis (OBIA), and deep learning (DL) for classifying coastal wetland vegetation from UAV RGB imagery highlight these advantages [119]. The PB method which relied mainly on spectral features, performed least effectively, while OBIA improved accuracy by incorporating spectral and texture features, reducing the "salt and pepper" effect (87.98% vs. 81.47%). DL achieved the highest accuracy (94.62%), automatically extracting complex spatial and structural features such as leaf forms and canopy patterns without manual input [119]. These findings underscore the potential of DL as a more robust and realistic approach to vegetation mapping, reinforcing its promise for fuel type classification in fire risk assessment and ecosystem management.

5. Integration of LFMC and Fuel Type into Fire Assessments

5.1. International Fire Risk Assessments

A fire risk assessment is an evaluation of fire hazards, likelihood of fire starting, and then if a fire does occur, what the consequences would be. Fuel models and fire behavior simulations are often used to evaluate the hazard (fire behavior potential). Fuel models are developed for individual fuel types based on their physical characteristics and the way they burn e.g., [120,121]. Depending on the individual fuel model, LFMC may be incorporated directly through foliar moisture content or grass curing, or indirectly through a drought factor.

Fire simulation models are mathematical and computational tools, that incorporate fuel models and are used to predict fire behavior (e.g., spread, growth, intensity). There are various empirical and dynamic wildfire simulators in use across the globe e.g., [122,123] and each of these simulators incorporate fuel moisture differently. In Appendix A, Table A1 we present a selection of wildfire simulation models and the associated fuel moisture inputs. In general fire simulation models use DFMC more dependably than LFMC (Table A1). Incorporation of DFMC is based on weather, fuel moisture indices, or pre-defined user functions (Table A1). The incorporation of LFMC is variable. Some models do not incorporate LFMC at all, while others incorporate LFMC based on specific fuel models or use a constant value (Table A1).

5.2. New Zealand Fire Risk Assessments

In New Zealand, fire risk assessments are part of the NZFDRS system. Development of the NZFDRS has largely focused on the Fire Weather Index (FWI) and the Fire Behaviour Prediction (FBP) subsystem modules (Figure 1). The FWI system is a weather-based system, which provides outputs associated with fuel moisture (primarily DFMC) and relative fire behavior potential. The Fire Occurrence Prediction (FOP) subsystem's objective is to provide information on the likelihood of ignitions occurring. In New Zealand this subsystem is currently in development through the creation of a wildfire occurrence database and ignition probability grids. The AFM subsystem's objective is to capture fuel moisture data for different fuels to complement the FWI system. This review and the subsequent pathway for implementation are the first steps towards the development and operation of an AFM subsystem for New Zealand.

The FBP subsystem is designed to provide estimates for rate of spread, consumption, and fire intensity for different fuel types. In New Zealand, these predictions of fire behavior are undertaken using a combination of tools including the Manual for Predicting Fire Behaviour in New Zealand Fuels, Fire Behaviour Toolkit [124] and the fire simulation models. In the early 2010's the Canadian wildland fire growth simulation model Prometheus [125] was reprogrammed to incorporate FWI inputs, fuel types, and fire behavior models specific to New Zealand. Prometheus is currently at end of life and the Wildfire Intelligence and Simulation Engine (W.I.S.E.) is the open-source replacement to Prometheus (firegrowthmodel.ca).

Fuel models are a foundational data input within fire behavior prediction systems, such as New Zealand's FBP subsystem. Fuel models are developed for individual fuel types based on their physical characteristics and the way they burn e.g., [120,121]. They provide the basic information necessary to forecast fire behavior (rate of spread, fire intensity) based on fuel properties (e.g., biomass, height). The development of fuel models in New Zealand, like the Canadian FBP System it is derived from, has been based on the correlation of FWI outputs with observed fire behavior from experimental burns and wildfires [28].

In Appendix A, Table A2 we present the existing and proposed New Zealand fuel types. In New Zealand, 18 fuel models have been developed to date for fire behavior predictions (Table A2). However, only 3 of these rate-of-spread models are used for the fire danger ratings: forest (mature pine plantation), shrub (scrublands include gorse and manuka), and grass (ungrazed pasture). New Zealand fuel models currently incorporate some stand level variation in forest structure (e.g., height, density) through the creation of individual age/stage models, with 6 of the 18 existing models representing different ages/stages of plantation fuels (Table A2).

Fuel models are linked to fuel type which is a critical input for the fire behavior prediction; however, appropriately scaled spatial and temporal fuels data are currently lacking for New Zealand. The Land Cover Database (LCDB) [126,127] is the best nationally available dataset but does not adequately distinguish fuel types relevant to fire behavior. For instance, the shrubs gorse (*Ulex europaeus*) and broom (*Cytisus scoparium*) are grouped under the same category, despite their differing fire behavior. Similarly, there is no distinction

for exotic forest areas based on species, age or stage. Moreover, the LCDB does not incorporate structural attributes such as canopy height or fuel load, which are essential for understanding fire propagation and intensity. Although the LCDB is periodically updated, its temporal frequency does not match the rate of landscape change, limiting its operational utility for forecasting dynamic fire risks.

Inputs for fire behavior prediction tools are often based on average fuel model values. The incorporation of near-real-time metrics provides an opportunity to move away from average model values, and through capturing landscape and stand level variation in LFMC, characterize fuel type, fuel load, and fuel height. In New Zealand, fire behavior simulations would be improved by incorporating near-real-time data into current tools, including the Fire Behaviour Toolkit calculator and W.I.S.E. Specifically, there is an opportunity to add data for fuel load, crown base height, crown fuel load, grass fuel load, foliar moisture content, and degree of curing. Although the degree of curing is not identical to fuel moisture, the LFMC decreases as grass cures and dies. Cured dead grasses have a DFMC of 2–35% while the LFMC of live, uncured or partially cured grasses ranges from 30–260% [128].

6. Pathway for Near-Real-Time Wildfire Risk Prediction Within New Zealand

Based on this review, we have identified a roadmap for the development of a near-real-time fuel moisture and fuel type system for New Zealand that can be integrated directly into the NZFDRS (Figure 4). As a standalone, a near-real-time fuel moisture monitoring system provides a critical risk management tool by identifying fuel moisture gradients in the landscape. Linking LFMC and fuel type directly to fire behavior models exponentially increases their value, improving fire behavior predictions and therefore opportunities to enhance wildfire risk management. Our overall objective is to enhance wildfire preparedness by improving our understanding of spatiotemporal wildfire hazards to allow better risk management decision making. The pathway forward has been defined by what is realistic from an operational standpoint, which differs from a purely research-driven perspective. Operational systems need to prioritize reliability, speed, and practical integration.

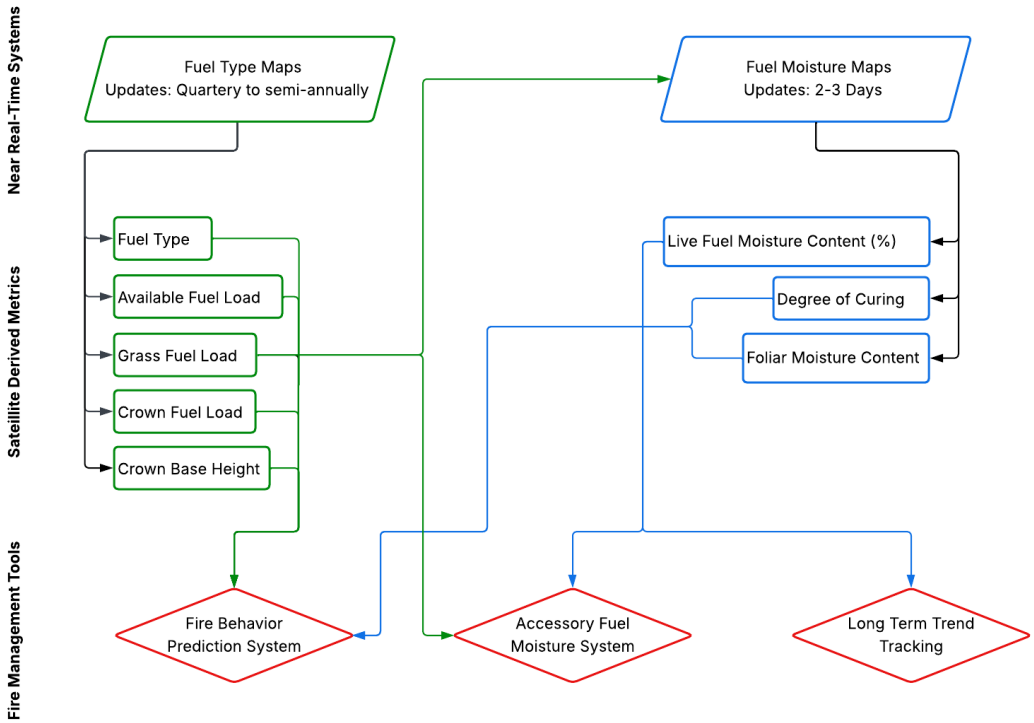


Figure 4. Diagram of how fuel type and fuel moisture spatial data products can be integrated directly into the NZFDRS.

6.1. Identification of Fuel Types

The goal of our fuel type modelling system is to create a robust classification of fuel types that captures both species composition and structural attributes. This mapping will be updated at a frequency suitable for monitoring fire-relevant changes (e.g., quarterly or bi-annually, depending on phenology).

Our first step in the development of a fuel model system was to identify the target fuel types. NZFDRS research has focused on the development of fuels models that are not part of the CFFDRS, such as shrub fuel types [129]. While there is some understanding around fire behavior in many fuel types, one of the reasons additional fuel models have not been developed is due to the uncertainty in the spatial distribution of these fuel types. An evaluation was completed to identify current and potential future fuel types. As part of this process, we identified 15 additional potential fuel types not represented in existing fuel models, bringing the total number of target fuel types to 33 when combined with the 18 models currently available (Table A2). For example, improved shrubland models were identified as a research priority [129], yet remain a research need, as do non-pasture grass and indigenous forest types.

Rather than creating individual fuel models for different ages and stages, we propose to incorporate structural data such as height and aboveground biomass into each fuel model. Structural data can be directly incorporated into FBP subsystem tools rather than using average values, improving fire behavior predictions. When individual age/stage models are removed from the existing fuel types, there are a total of 24 current and proposed fuel types to be identified with fuel type modelling (Table A2).

Each classification method reviewed to date has associated strengths and weaknesses. Pixel-based methods are simpler to implement, but New Zealand's highly heterogeneous landscapes require approaches that can accurately classify small-scale variation in fuel types. As spatial resolution becomes coarser, classification accuracy deteriorates in fire-relevant applications, because fire behavior is sensitive to the spatial arrangement and connectivity of fuels.

Spectral mixture analysis, which estimates the fractional composition of different fuels within a pixel, offers an alternative, but is limited by the availability of reliable endmembers across complex landscapes. Conversely, object-based image analysis (OBIA) methods, especially when implemented via deep learning, provide better performance in heterogeneous environments by leveraging textural and contextual information. Given these advantages, we propose an OBIA or deep learning approach for New Zealand, with deep learning preferred for its scalability and efficiency.

Figure 5 outlines the proposed workflow for establishing a national fuel type classification. The process begins with very high-resolution (VHR) optical imagery, used for a one-time baseline map that provides training data for deep learning models. These models can then be applied to more routinely available datasets such as HLS, Sentinel-1, and GEDI (where available, with operations planned through 2030), integrating both spectral and structural inputs to enable consistent, large-scale mapping.

Training data will be derived through manual delineation of fuel type polygons, informed by existing species-specific maps (e.g., ForestInsights) and citizen science resources such as Global Biodiversity Information Facility (GBIF) occurrence records, and validated through targeted field visits. Structural information from LiDAR and Sentinel-1 will also be incorporated to improve classification performance, feeding into the iterative update of fuel type maps.

Ultimately, this new classification system will form a foundational input for near-real-time fuel moisture and fire behavior models. Its development is critical for creating a dynamic, operational fire assessment system that reflects actual vegetation and fuel

conditions, enabling better planning and incident response. This system will also address the limitations of static land cover datasets and contribute to broader ecological monitoring beyond wildfire management, such as a monitoring system to track land use change.

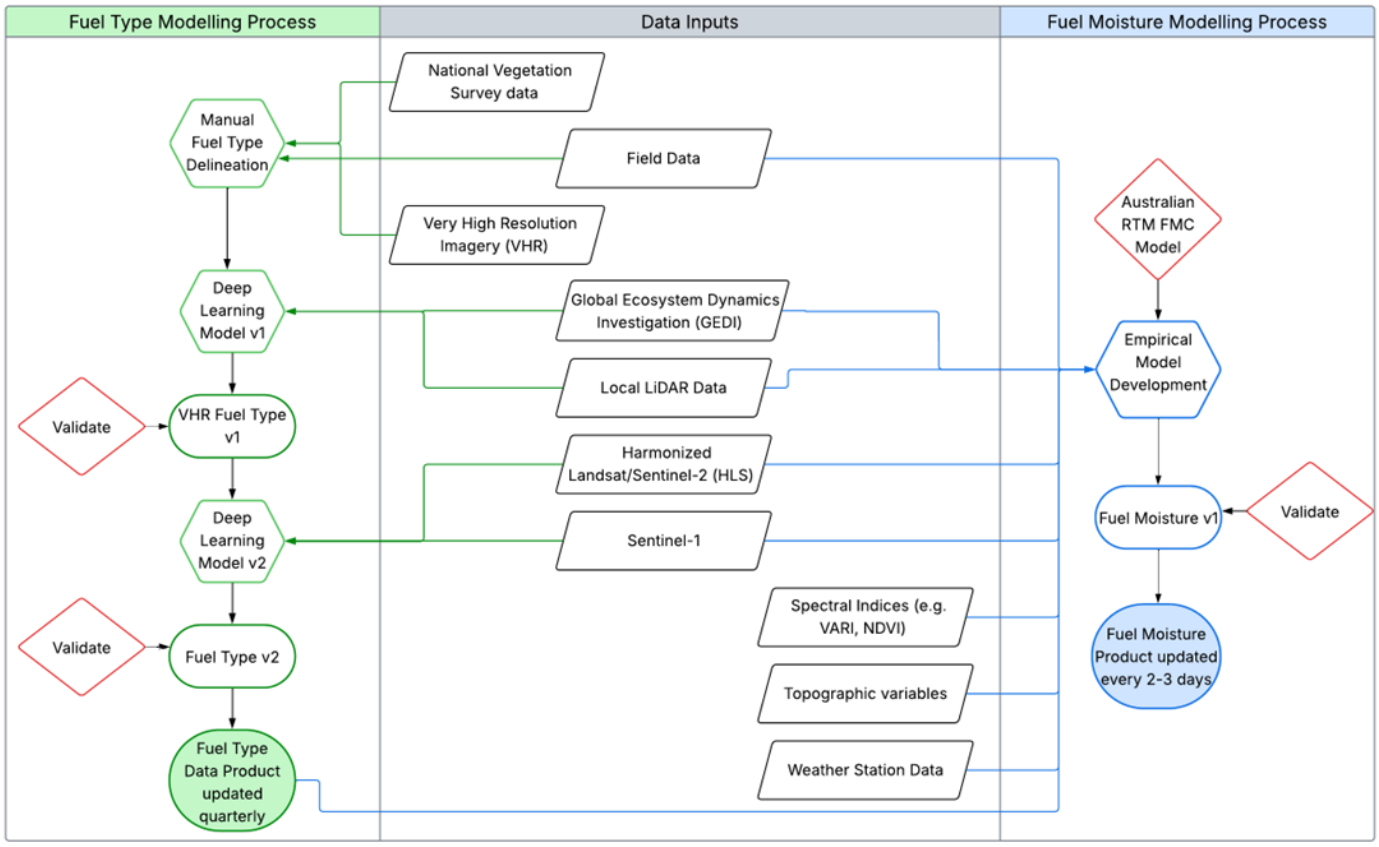


Figure 5. Process diagram to develop remotely sensed fuel type maps with quarterly updates (left) and fuel moisture maps with 2–3 day updates (right). Both products will be incorporated into wildfire assessments (Figure 4). References are given in brackets for the National Vegetation Survey data [130] and Australian RTM FMC Model [111].

6.2. Prediction of LFMC

The goal of our live fuel moisture content model is to create a near-real-time fuel moisture system that can be updated every 2–3 days to capture fuel moisture changes that occur across the landscape. The LFMC system can also contribute to broader ecological monitoring beyond wildfire by creating a system to provide localised drought warnings based on long-term anomaly tracking.

Numerous studies have shown that combining SAR with optical data improves LFMC model accuracy [71,81]. These findings strongly support the integration of complementary datasets for robust LFMC prediction. We propose the development of an operational LFMC prediction system for New Zealand that integrates Sentinel-1 with the Harmonized Landsat and Sentinel-2 (HLS) multispectral dataset (Figure 5). This hybrid approach addresses one of New Zealand's key remote sensing challenges, persistent cloud cover, by leveraging the cloud-penetrating capabilities of SAR alongside the spectral richness of multispectral imagery.

The frequent, harmonized observations enable fine temporal resolution for detecting changes in fuel moisture while maintaining adequate spatial detail. Additionally, as HLS is built on the long-term Landsat and Sentinel-2 archives, historical comparisons and validations of fuel moisture during past characterized fire events will be possible.

To strengthen LFMC prediction further, we will incorporate ancillary information into predictive models. Fuel type and stand structural attributes, such as canopy height and vegetation fractional cover, influence both fire behavior and LFMC dynamics. Their inclusion has been shown to significantly improve model accuracy [78]. We will also explore the integration of weather variables, which are key to capturing short-term moisture fluctuations. Variables such as cumulative precipitation, temperature (including land surface temperature and 30–60 day temperature aggregates), and wind speed have all been shown to enhance model performance depending on landscape context [79,104,105]. LFMC sampling will be located near operational meteorological stations.

As such, we propose a dual-pathway approach (Figure 5). First, we will develop a New Zealand-specific empirical LFMC model using spectral indices derived from HLS and Sentinel-1 data in addition to ancillary information. Empirical models offer high operational efficiency, are straightforward to implement, and require fewer computational resources making them attractive for real-time systems (Table 2). These models will be calibrated with LFMC field data from a pilot study covering three distinct fuel types—forest, shrub, and grassland—representing the fuel models used in fire danger classes across different climatic zones. This design will allow us to assess sampling requirements, optimize spectral indices and ancillary data selection, and evaluate model performance across fuel types and regions.

Table 2. Summary of the strengths and weaknesses of empirical, machine learning (ML), and physical models for estimating LFMC. Traits considered to be positive for the development of an operational system are denoted with bold text.

Attribute	Model Type		
	Empirical	**ML**	**Physical**
Computational requirements	**Low**	High	High
Generalizability across various conditions	Low	Low	**High**
Requires understanding of physical variables	**Low**	**Low**	High
Parameterization	**Low**	**Low**	High
Interpretability	**High**	Low	**High**
Complexity	**Low**	High	High

Second, we will use the Australian RTM-based LFMC model in parallel as a benchmark to validate our empirical results and assess whether physically based modelling offers greater generality than empirical approaches (Table 2). The broader applicability of RTM-based methods is evidenced by their successful use in accurately predicting FMC across diverse vegetation types in Australia [111] and globally [113]. Recent research [131] has also shown that the physical model developed for Australian ecosystems outperformed machine learning models when transferred to Mediterranean environments in Israel, suggesting good cross-ecosystem transferability. This comparative approach will inform decisions around model transferability and guide whether to adapt or locally recalibrate the RTM model for New Zealand (Figure 5).

7. Conclusions

This study synthesized current knowledge on remote sensing-based approaches for estimating live fuel moisture content (LFMC), with the goal of informing the development of an operational prediction system for New Zealand. Insights drawn from the synthesis in Table 1 were used to identify the most operationally promising sensors and modelling frameworks, forming the evidence base for the proposed implementation pathway. As climate change increases the frequency and severity of wildfires, the need for reliable,

timely LFMC estimates has become more urgent. While satellite-derived LFMC estimation has advanced considerably in recent years, practical implementation for New Zealand remains constrained by factors such as limited field data, variable sensor performance across fuel types, and the absence of fit-for-purpose fuel classification products.

Our review highlights that no single modelling approach for predicting LFMC is universally optimal; rather, the choice depends on regional data availability, vegetation characteristics, and operational constraints. Empirical models offer simplicity and computational efficiency, machine learning approaches enable flexible integration of diverse data streams, and physical models provide strong generalizability across ecosystems. However, effective LFMC estimation also hinges on accurate fuel-type mapping and the ability to resolve temporal changes in vegetation moisture at scales relevant to fire risk. In the New Zealand context, persistent cloud cover and complex terrain necessitate an approach that integrates both optical and microwave satellite observations.

To address these challenges, we propose a staged pilot study to evaluate LFMC estimation methods across representative fuel types and climate zones. This will allow the calibration and validation of models under varying conditions, while also testing the operational feasibility of near-real-time implementation. The insights gained from this work will guide the establishment of a scalable, satellite-based LFMC monitoring system tailored to New Zealand's unique fire environment. Beyond New Zealand, the framework developed here may inform similar efforts in other fire-prone, data-limited regions facing growing wildfire risk.

Author Contributions: Conceptualization, M.S.W., S.G., J.K.D., J.L.M., H.G.P., J.K.S. and M.Y.; methodology, M.S.W., S.G., J.K.D., J.L.M., H.G.P., J.K.S. and M.Y.; formal analysis, J.K.D., M.S.W. and S.G.; investigation, J.K.D., M.S.W. and S.G.; resources, S.G.; data curation, J.K.D., M.S.W. and S.G.; writing—original draft preparation, M.S.W., J.K.D. and S.G.; writing—review and editing, M.S.W., S.G., J.K.D., J.L.M., H.G.P., J.K.S. and M.Y.; visualization, M.S.W., S.G., J.K.D., J.L.M. and M.Y.; supervision, S.G.; project administration, S.G.; funding acquisition, S.G. All authors have read and agreed to the published version of the manuscript.

Funding: This research was funded by the Ministry of Business, Innovation and Employment (MBIE) under contracts C04X1703, C04X2303 and FRI2424.

Data Availability Statement: No new data were created or analyzed in this study. Data sharing is not applicable to this article.

Conflicts of Interest: The authors declare no conflicts of interest.

Abbreviations

The following abbreviations are used in this manuscript:

AFM	Accessory Fuel Moisture
ALS	Airborne Laser Scanning
AVIRIS	Airborne Visible/Infrared Imaging Spectrometer
CFFDRS	Canadian Fire Danger System
CNN	Convolutional Neural Networks
DEM	Digital elevation model
DFMC	Dead fuel moisture content
DL	Deep learning
FBP	Fire Behavior Prediction
FMC	Fuel Moisture Content
FOP	Fire Occurrence Prediction
FWI	Fire Weather Index

GAM	Generalized additive models
GEDI	Global Ecosystem Dynamics Investigation
GOES	Geostationary Operational Environmental Satellite
GPU	Graphics Processing Units
GSD	Ground Sampling Distance
GVMI	Global Vegetation Moisture Index
HLS	Harmonized Landsat and Sentinel-2 dataset
LAI	Leaf area index
LFMC	Live fuel moisture content
LiDAR	Light detection and ranging
MIVIS	Multispectral Infrared and Visible Imaging Spectrometer
ML	Machine learning
MLR	Multivariate linear regression
MODIS	Moderate Resolution Imaging Spectroradiometer
MSI	Moisture Stress Index
NDVI	Normalized Difference Vegetation Index
NIR	Near-infrared
NLR	Non-linear regression
NZFDRS	New Zealand Fire Danger Rating System
OA	Overall accuracy
OBIA	Object-based image analysis
PB	Pixel based
RF	Random forest
RTM	Radiative transfer model
SAR	Synthetic aperture radar
SMA	Spectral Mixture Analysis
SWIR	Shortwave infrared
TIR	Thermal infrared
VARI	Visible Atmospherically Resistant Index
VHR	Very high resolution satellites
VIIRS	Visible Infrared Imaging Radiometer Suite
VIS	Visible
VNIR	Visible and Near-Infrared

Appendix A

Table A1. Selected wildfire simulation models and associated fuel moisture inputs.

Country	Fire Behavior Simulator *	Description	LFMC	DFMC
Australia	Spark [132]	Toolkit for the end-to-end processing, simulation and analysis of wildfires.	Variable based on specific fuel model: percent curing, percent live and dead, moisture content of extinction	Pre-defined user effect function
Australia (southern and eastern)	Phoenix Rapidfire [133].	Wildfire simulation for operational and preparedness—fire risk modelling.	Grass fuel moisture is based on a grass function	Fine fuel moisture model is incorporated based on weather. Coarse woody fuel consumption based on a drought factor (DF)
Canada, New Zealand	Prometheus [125]; W.I.S.E. (Wildfire Intelligence and Simulation Engine)	Deterministic wildland fire growth simulation model based on Fire Weather Index (FWI) and Fire Behavior Prediction (FBP) systems.	FMC—foliar moisture content (FBP input for forest fuel types: for Canada, FMC based on latitude, longitude, elevation, and date and can vary 85–120%; in NZ default is 145% all year); grass curing	Based on FWI fuel moisture codes (FFMC, DMC, DC)

Table A1. *Cont.*

Country	Fire Behavior Simulator *	Description	LFMC	DFMC
USA	WFDS (Wildland-Urban Interface Fire Dynamics Simulator) [134]	Computational fluid dynamics model to solve the governing equations for buoyant flow, heat transfer, combustion, and the thermal degradation of vegetative fuels.	Foliage crown and branch crown moisture inputs	Surface fuel moisture input
USA	FlamMap (& FARSITE) [135,136]	Simulates wildfire behavior for fuel treatment planning.	Constant	Based on weather inputs
USA	FSim [137]	Wildfire risk simulation software that calculates annual probabilities of burning and fire line intensity distributions at various points on the landscape.	None	Distribution of fuel moisture based on weather inputs
Sweden, Indonesia, South Korea, Italy, and Austria	FLAM (wild**F**ire c**L**imate impacts and **A**daptation **M**odel) e.g., [138]	Process-based fire parameterization algorithm linking a fire simulation model with dynamic global vegetation models for planning purposes.	None	FFMC from FWI

* Selected fire simulators from around the world (this is not an extensive list of simulation software) to demonstrate how fuel moisture metrics are incorporated into fire simulations.

Table A2. Existing and proposed New Zealand fuel types.

Status	Fire Danger Class	Fuel Type	NZ Fire Behaviour Prediction (FBP) Fuel Model	NZ FBP Group [1]
Proposed	Forest	Exotic Forest	Wilding Pine	
Existing	Forest	Indigenous Forests	Beech Forests	
Existing	Forest	Indigenous Forests	Podocarp/Broadleaf	
Proposed	Forest	Indigenous Forests	Broadleaf forest	
Proposed	Forest	Indigenous Forests	Mixed Beech/Broadleaf Forest	
Proposed	Forest	Indigenous Forests	Mixed Beech/Podocarp/Broadleaf Forest	
Existing	Forest	Plantation Forests	Immature Pine 1–4 years old (1st rotation)	Pine Plantation
Existing	Forest	Plantation Forests	Immature Pine 1–4 years old (2nd rotation)	Pine Plantation
Existing	Forest	Plantation Forests	Immature Pine 5–10 years old	Pine Plantation
Existing	Forest	Plantation Forests	Immature pine 11–20 years old	Pine Plantation
Existing	Forest	Plantation Forests	Mature Pine 20+ years old	Pine Plantation
Existing	Forest	Plantation Forests	Plantation Forest Slash	Pine Plantation
Proposed	Forest	Plantation Forests	Shelter Belts and Hedges	Pine Plantation
Proposed	Forest	Plantation Forests	Douglas-fir	
Proposed	Forest	Plantation Forests	Eucalypts	
Existing	Grass	Crop Stubble	Baled stubble	Stubble
Existing	Grass	Crop Stubble	Unbaled stubble	Stubble
Existing	Grass	Pasture Grasslands	Grazed Pasture	Pasture
Existing	Grass	Pasture Grasslands	Ungrazed Pasture	Pasture
Proposed	Grass	Pasture Grasslands	Orchard, Vineyard	
Proposed	Grass	Peatland	Peatland	
Existing	Grass	Tussock Grasslands	Grazed Tussock	Tussock
Existing	Grass	Tussock Grasslands	Ungrazed Tussock	Tussock
Proposed	Grass	Tussock Grasslands	Beach Grasses	
Proposed	Other	Non-Fuel	Non-burnable	
Proposed	Other	Non-vegetation	Refuse Dumps	
Proposed	Other	Non-vegetation	Rural Urban Interface	
Existing	Scrub	Scrublands	Gorse	
Existing	Scrub	Scrublands	Heathlands/Wetlands	
Existing	Scrub	Scrublands	Manuka/Kanuka	
Existing	Scrub	Scrublands	Hardwood Shrubs	
Proposed	Scrub	Scrublands	Broom	
Proposed	Scrub	Scrublands	Sub-alpine Shrubs	

[1] The NZ FBP group refers to where there are currently several models for a fuel type based on fuel structural characteristics which could be reduced to a single fuel model when structural data is incorporated.

References

1. Andela, N.; Morton, D.C.; Giglio, L.; Paugam, R.; Chen, Y.; Hantson, S.; Van Der Werf, G.R.; Randerson, J.T. The Global Fire Atlas of individual fire size, duration, speed and direction. *Earth Syst. Sci. Data* **2019**, *11*, 529–552. [CrossRef]
2. Jones, M.W.; Abatzoglou, J.T.; Veraverbeke, S.; Andela, N.; Lasslop, G.; Forkel, M.; Smith, A.J.; Burton, C.; Betts, R.A.; van der Werf, G.R. Global and regional trends and drivers of fire under climate change. *Rev. Geophys.* **2022**, *60*, e2020RG000726. [CrossRef]
3. Bowman, D.M.; Kolden, C.A.; Abatzoglou, J.T.; Johnston, F.H.; van der Werf, G.R.; Flannigan, M. Vegetation fires in the Anthropocene. *Nat. Rev. Earth Environ.* **2020**, *1*, 500–515. [CrossRef]
4. Dupuy, J.-l.; Fargeon, H.; Martin-StPaul, N.; Pimont, F.; Ruffault, J.; Guijarro, M.; Hernando, C.; Madrigal, J.; Fernandes, P. Climate change impact on future wildfire danger and activity in southern Europe: A review. *Ann. For. Sci.* **2020**, *77*, 35. [CrossRef]
5. de Dios, V.R.; Hedo, J.; Camprubí, À.C.; Thapa, P.; Del Castillo, E.M.; de Aragón, J.M.; Bonet, J.A.; Balaguer-Romano, R.; Díaz-Sierra, R.; Yebra, M. Climate change induced declines in fuel moisture may turn currently fire-free Pyrenean mountain forests into fire-prone ecosystems. *Sci. Total Environ.* **2021**, *797*, 149104. [CrossRef]
6. Watt, M.S.; Kirschbaum, M.U.F.; Moore, J.R.; Pearce, H.G.; Bulman, L.S.; Brockerhoff, E.G.; Melia, N. Assessment of multiple climate change effects on plantation forests in New Zealand. *For. Int. J. For. Res.* **2019**, *92*, 1–15. [CrossRef]
7. Stats, N.Z. Wildfire Risk: Data to 2023. Available online: https://www.stats.govt.nz/indicators/wildfire-risk-data-to-2023/ (accessed on 31 August 2025).
8. Wastl, C.; Schunk, C.; Lüpke, M.; Cocca, G.; Conedera, M.; Valese, E.; Menzel, A. Large-scale weather types, forest fire danger, and wildfire occurrence in the Alps. *Agric. For. Meteorol.* **2013**, *168*, 15–25. [CrossRef]
9. Janizadeh, S.; Bateni, S.M.; Jun, C.; Im, J.; Pai, H.-T.; Band, S.S.; Mosavi, A. Combination four different ensemble algorithms with the generalized linear model (GLM) for predicting forest fire susceptibility. *Geomat. Nat. Hazards Risk* **2023**, *14*, 2206512. [CrossRef]
10. Chuvieco, E.; Yebra, M.; Martino, S.; Thonicke, K.; Gómez-Giménez, M.; San-Miguel, J.; Oom, D.; Velea, R.; Mouillot, F.; Molina, J.R.; et al. Towards an Integrated Approach to Wildfire Risk Assessment: When, Where, What and How May the Landscapes Burn. *Fire* **2023**, *6*, 215. [CrossRef]
11. Yebra, M.; Dennison, P.E.; Chuvieco, E.; Riaño, D.; Zylstra, P.; Hunt Jr, E.R.; Danson, F.M.; Qi, Y.; Jurdao, S. A global review of remote sensing of live fuel moisture content for fire danger assessment: Moving towards operational products. *Remote Sens. Environ.* **2013**, *136*, 455–468. [CrossRef]
12. Viegas, D.X.; Viegas, M.; Ferreira, A. Moisture content of fine forest fuels and fire occurrence in central Portugal. *Int. J. Wildland Fire* **1992**, *2*, 69–86. [CrossRef]
13. Viegas, D.; Viegas, M.; Ferreira, A. Characteristics of some forest fuels and their relation to the occurence of fires. In Proceedings of the International Conference of Forest Fire Research, Coimbra, Portugal, 19–22 November 1990; pp. 1–13.
14. Xanthopoulos, G.; Wakimoto, R.H. A time to ignition–temperature–moisture relationship for branches of three western conifers. *Can. J. For. Res.* **1993**, *23*, 253–258. [CrossRef]
15. García, M.; Riaño, D.; Yebra, M.; Salas, J.; Cardil, A.; Monedero, S.; Ramirez, J.; Martín, M.P.; Vilar, L.; Gajardo, J. A live fuel moisture content product from Landsat TM satellite time series for implementation in fire behavior models. *Remote Sens.* **2020**, *12*, 1714. [CrossRef]
16. Schoenberg, F.P.; Peng, R.; Huang, Z.; Rundel, P. Detection of non-linearities in the dependence of burn area on fuel age and climatic variables. *Int. J. Wildland Fire* **2003**, *12*, 1–6. [CrossRef]
17. Dennison, P.E.; Moritz, M.A. Critical live fuel moisture in chaparral ecosystems: A threshold for fire activity and its relationship to antecedent precipitation. *Int. J. Wildland Fire* **2009**, *18*, 1021–1027. [CrossRef]
18. Dennison, P.E.; Moritz, M.A.; Taylor, R.S. Evaluating predictive models of critical live fuel moisture in the Santa Monica Mountains, California. *Int. J. Wildland Fire* **2008**, *17*, 18–27. [CrossRef]
19. Anderson, S.A.; Anderson, W.R. Ignition and fire spread thresholds in gorse (Ulex europaeus). *Int. J. Wildland Fire* **2010**, *19*, 589–598. [CrossRef]
20. Plucinski, M.P.; Anderson, W.R.; Bradstock, R.A.; Gill, A.M. The initiation of fire spread in shrubland fuels recreated in the laboratory. *Int. J. Wildland Fire* **2010**, *19*, 512–520. [CrossRef]
21. Nolan, R.H.; Boer, M.M.; Resco de Dios, V.; Caccamo, G.; Bradstock, R.A. Large-scale, dynamic transformations in fuel moisture drive wildfire activity across southeastern Australia. *Geophys. Res. Lett.* **2016**, *43*, 4229–4238. [CrossRef]
22. Pimont, F.; Ruffault, J.; Martin-StPaul, N.; Dupuy, J.-L. A cautionary note regarding the use of cumulative burnt areas for the determination of fire danger index breakpoints. *Int. J. Wildland Fire* **2019**, *28*, 254–258. [CrossRef]
23. Yebra, M.; Scortechini, G.; Adeline, K.; Aktepe, N.; Almoustafa, T.; Bar-Massada, A.; Beget, M.E.; Boer, M.; Bradstock, R.; Brown, T. Globe-LFMC 2.0, an enhanced and updated dataset for live fuel moisture content research. *Sci. Data* **2024**, *11*, 332. [CrossRef]
24. Dennison, P.E.; Roberts, D.A.; Thorgusen, S.R.; Regelbrugge, J.C.; Weise, D.; Lee, C. Modeling seasonal changes in live fuel moisture and equivalent water thickness using a cumulative water balance index. *Remote Sens. Environ.* **2003**, *88*, 442–452. [CrossRef]

25. Jurdao, S.; Yebra, M.; Guerschman, J.P.; Chuvieco, E. Regional estimation of woodland moisture content by inverting Radiative Transfer Models. *Remote Sens. Environ.* **2013**, *132*, 59–70. [CrossRef]
26. Stow, D.; Niphadkar, M.; Kaiser, J. MODIS-derived visible atmospherically resistant index for monitoring chaparral moisture content. *Int. J. Remote Sens.* **2005**, *26*, 3867–3873. [CrossRef]
27. Ruffault, J.; Martin-StPaul, N.; Pimont, F.; Dupuy, J.-L. How well do meteorological drought indices predict live fuel moisture content (LFMC)? An assessment for wildfire research and operations in Mediterranean ecosystems. *Agric. For. Meteorol.* **2018**, *262*, 391–401. [CrossRef]
28. Anderson, S. Forest and rural fire danger rating in New Zealand. In *Forestry Handbook*; Colley, M., Ed.; New Zealand Institute of Forestry: Christchurch, New Zealand, 2005; pp. 241–244.
29. Wotton, M. A grass moisture model for the Canadian forest fire danger rating system. In Proceedings of the Eighth Symposium on Fire and Forest Meteorology, Kalispell, MT, USA, 12–15 October 2009; American Meteorological Society: Boston, NE, USA, 2009.
30. Van Wagner, C. *A Method of Computing Fine Fuel Moisture Content Throughout the Diurnal Cycle*; Environment Canada, Canadian Forestry Service, Petawawa Forest Experiment Station: Chalk River, ON, USA, 1977.
31. Chuvieco, E.; Aguado, I.; Salas, J.; García, M.; Yebra, M.; Oliva, P. Satellite remote sensing contributions to wildland fire science and management. *Curr. For. Rep.* **2020**, *6*, 81–96. [CrossRef]
32. Arroyo, L.A.; Pascual, C.; Manzanera, J.A. Fire models and methods to map fuel types: The role of remote sensing. *For. Ecol. Manag.* **2008**, *256*, 1239–1252. [CrossRef]
33. Abdollahi, A.; Yebra, M. Forest fuel type classification: Review of remote sensing techniques, constraints and future trends. *J. Environ. Manag.* **2023**, *342*, 118315. [CrossRef] [PubMed]
34. Ustin, S.L.; Middleton, E.M. Current and near-term advances in Earth observation for ecological applications. *Ecol. Process.* **2021**, *10*, 1. [CrossRef]
35. Whitcraft, A.K.; Vermote, E.F.; Becker-Reshef, I.; Justice, C.O. Cloud cover throughout the agricultural growing season: Impacts on passive optical earth observations. *Remote Sens. Environ.* **2015**, *156*, 438–447. [CrossRef]
36. Zarco-Tejada, P.J.; González-Dugo, V.; Berni, J.A.J. Fluorescence, temperature and narrow-band indices acquired from a UAV platform for water stress detection using a micro-hyperspectral imager and a thermal camera. *Remote Sens. Environ.* **2012**, *117*, 322–337. [CrossRef]
37. Scherrer, D.; Bader, M.K.-F.; Körner, C. Drought-sensitivity ranking of deciduous tree species based on thermal imaging of forest canopies. *Agric. For. Meteorol.* **2011**, *151*, 1632–1640. [CrossRef]
38. Seidel, H.; Schunk, C.; Matiu, M.; Menzel, A. Diverging drought resistance of scots pine provenances revealed by infrared thermography. *Front. Plant Sci.* **2016**, *7*, 1247. [CrossRef] [PubMed]
39. Still, C.; Powell, R.; Aubrecht, D.; Kim, Y.; Helliker, B.; Roberts, D.; Richardson, A.D.; Goulden, M. Thermal imaging in plant and ecosystem ecology: Applications and challenges. *Ecosphere* **2019**, *10*, e02768. [CrossRef]
40. Chandra, S.N.R.; Christopherson, J.B.; Casey, K.A.; Lawson, J.; Sampath, A. *2022 Joint Agency Commercial Imagery Evaluation—Remote Sensing Satellite Compendium*; U.S. Geological Survey Circular 1500; Geological Survey: Reston, VA, USA, 2022; 279p. Available online: https://pubs.usgs.gov/publication/cir1500 (accessed on 20 August 2025).
41. Smigaj, M.; Agarwal, A.; Bartholomeus, H.; Decuyper, M.; Elsherif, A.; de Jonge, A.; Kooistra, L. Thermal Infrared Remote Sensing of Stress Responses in Forest Environments: A Review of Developments, Challenges, and Opportunities. *Curr. For. Rep.* **2024**, *10*, 56–76. [CrossRef]
42. Xie, J.; Qi, T.; Hu, W.; Huang, H.; Chen, B.; Zhang, J. Retrieval of Live Fuel Moisture Content Based on Multi-Source Remote Sensing Data and Ensemble Deep Learning Model. *Remote Sens.* **2022**, *14*, 4378. [CrossRef]
43. Rao, K.; Williams, A.P.; Flefil, J.F.; Konings, A.G. SAR-enhanced mapping of live fuel moisture content. *Remote Sens. Environ.* **2020**, *245*, 111797. [CrossRef]
44. Alonso-Benito, A.; Arroyo, L.A.; Arbelo, M.; Hernández-Leal, P. Fusion of WorldView-2 and LiDAR data to map fuel types in the Canary Islands. *Remote Sens.* **2016**, *8*, 669. [CrossRef]
45. García, M.; Riaño, D.; Chuvieco, E.; Salas, J.; Danson, F.M. Multispectral and LiDAR data fusion for fuel type mapping using Support Vector Machine and decision rules. *Remote Sens. Environ.* **2011**, *115*, 1369–1379. [CrossRef]
46. Chirici, G.; Scotti, R.; Montaghi, A.; Barbati, A.; Cartisano, R.; Lopez, G.; Marchetti, M.; McRoberts, R.E.; Olsson, H.; Corona, P. Stochastic gradient boosting classification trees for forest fuel types mapping through airborne laser scanning and IRS LISS-III imagery. *Int. J. Appl. Earth Obs. Geoinf.* **2013**, *25*, 87–97. [CrossRef]
47. Domingo, D.; de la Riva, J.; Lamelas, M.T.; García-Martín, A.; Ibarra, P.; Echeverría, M.; Hoffrén, R. Fuel type classification using airborne laser scanning and Sentinel 2 data in Mediterranean forest affected by wildfires. *Remote Sens.* **2020**, *12*, 3660. [CrossRef]
48. Zhu, Y.; Liu, X.; Lai, G.; Quan, X. Evaluation of Himawari-8 for live fuel moisture content retrieval. In Proceedings of the IGARSS 2020—2020 IEEE International Geoscience and Remote Sensing Symposium, Waikoloa, HI, USA, 26 September–2 October 2020.
49. Quan, X.; Chen, R.; Yebra, M.; Riaño, D.; de Dios, V.R.; Li, X.; He, B.; Nolan, R.H.; Griebel, A.; Boer, M.M. Sub-daily live fuel moisture content estimation from Himawari-8 data. *Remote Sens. Environ.* **2024**, *308*, 114170. [CrossRef]

50. Zawadzki, J.; Cieszewski, C.J.; Zasada, M.; Lowe, R.C. Applying geostatistics for investigations of forest ecosystems using remote sensing imagery. *Silva Fenn.* **2005**, *39*, 599–617. [CrossRef]
51. Lee, J.-H.; Sull, S. Regression tree CNN for estimation of ground sampling distance based on floating-point representation. *Remote Sens.* **2019**, *11*, 2276. [CrossRef]
52. Knipling, E.B. Physical and physiological basis for the reflectance of visible and near-infrared radiation from vegetation. *Remote Sens. Environ.* **1970**, *1*, 155–159. [CrossRef]
53. Thomas, J.R.; Namken, L.N.; Oerther, G.F.; Brown, R.G. Estimating Leaf Water Content by Reflectance Measurements 1. *Agron. J.* **1971**, *63*, 845–847. [CrossRef]
54. Tucker, C.J. Remote sensing of leaf water content in the near infrared. *Remote Sens. Environ.* **1980**, *10*, 23–32. [CrossRef]
55. Fourty, T.; Baret, F. Vegetation water and dry matter contents estimated from top-of-the-atmosphere reflectance data: A simulation study. *Remote Sens. Environ.* **1997**, *61*, 34–45.
56. Datt, B. Remote sensing of water content in Eucalyptus leaves. *Aust. J. Bot.* **1999**, *47*, 909–923. [CrossRef]
57. Danson, F.M.; Bowyer, P. Estimating live fuel moisture content from remotely sensed reflectance. *Remote Sens. Environ.* **2004**, *92*, 309–321. [CrossRef]
58. Colombo, R.; Meroni, M.; Marchesi, A.; Busetto, L.; Rossini, M.; Giardino, C.; Panigada, C. Estimation of leaf and canopy water content in poplar plantations by means of hyperspectral indices and inverse modeling. *Remote Sens. Environ.* **2008**, *112*, 1820–1834. [CrossRef]
59. Peterson, S.H.; Roberts, D.A.; Dennison, P.E. Mapping live fuel moisture with MODIS data: A multiple regression approach. *Remote Sens. Environ.* **2008**, *112*, 4272–4284. [CrossRef]
60. García, M.; Chuvieco, E.; Nieto, H.; Aguado, I. Combining AVHRR and meteorological data for estimating live fuel moisture content. *Remote Sens. Environ.* **2008**, *112*, 3618–3627. [CrossRef]
61. Vermunt, P. Understanding Radar Backscatter Sensitivity to Vegetation Water Dynamics: Sub-Daily Variations in Ground-Based Experiments. Ph.D. Thesis, Delft University of Technology, Delft, The Netherlands, 2022.
62. Way, J.; Paris, J.; Dobson, M.C.; McDonals, K.; Ulaby, F.T.; Weber, J.; Ustin, L.; Vanderbilt, V.C.; Kasischke, E.S. Diurnal change in trees as observed by optical and microwave sensors: The EOS synergism study. *IEEE Trans. Geosci. Remote Sens.* **1991**, *29*, 807–821. [CrossRef]
63. Beaudoin, A.; Vidal, A.; Desbois, N.; Devaux-Ros, C. Monitoring the water status of Mediterranean forests using ERS-1, to support fire risk prevention. In Proceedings of the 1995 International Geoscience and Remote Sensing Symposium, IGARSS'95. Quantitative Remote Sensing for Science and Applications, Florence, Italy, 10–14 July 1995.
64. Schmidt, L.; Forkel, M.; Zotta, R.-M.; Scherrer, S.; Dorigo, W.A.; Kuhn-Régnier, A.; Van Der Schalie, R.; Yebra, M. Assessing the sensitivity of multi-frequency passive microwave vegetation optical depth to vegetation properties. *Biogeosci. Discuss.* **2022**, *2022*, 1–24. [CrossRef]
65. Chuvieco, E.; Cocero, D.; Riano, D.; Martin, P.; Martınez-Vega, J.; De La Riva, J.; Pérez, F. Combining NDVI and surface temperature for the estimation of live fuel moisture content in forest fire danger rating. *Remote Sens. Environ.* **2004**, *92*, 322–331. [CrossRef]
66. Dennison, P.; Roberts, D.A.; Peterson, S.H.; Rechel, J. Use of normalized difference water index for monitoring live fuel moisture. *Int. J. Remote Sens.* **2005**, *26*, 1035–1042. [CrossRef]
67. Hao, X.; Qu, J.J. Retrieval of real-time live fuel moisture content using MODIS measurements. *Remote Sens. Environ.* **2007**, *108*, 130–137. [CrossRef]
68. Yebra, M.; Chuvieco, E.; Riano, D. Estimation of live fuel moisture content from MODIS images for fire risk assessment. *Agric. For. Meteorol.* **2008**, *148*, 523–536. [CrossRef]
69. Caccamo, G.; Chisholm, L.; Bradstock, R.; Puotinen, M.L.; Pippen, B. Monitoring live fuel moisture content of heathland, shrubland and sclerophyll forest in south-eastern Australia using MODIS data. *Int. J. Wildland Fire* **2011**, *21*, 257–269. [CrossRef]
70. Al-Moustafa, T.; Armitage, R.P.; Danson, F.M. Mapping fuel moisture content in upland vegetation using airborne hyperspectral imagery. *Remote Sens. Environ.* **2012**, *127*, 74–83. [CrossRef]
71. Fan, L.; Wigneron, J.-P.; Xiao, Q.; Al-Yaari, A.; Wen, J.; Martin-StPaul, N.; Dupuy, J.-L.; Pimont, F.; Al Bitar, A.; Fernandez-Moran, R. Evaluation of microwave remote sensing for monitoring live fuel moisture content in the Mediterranean region. *Remote Sens. Environ.* **2018**, *205*, 210–223. [CrossRef]
72. Marino, E.; Guillén-Climent, M.; Algeet, N.; Tomé, J.L.; Hernando, C. Estimation of Live Fuel Moisture Content of Shrubland Using MODIS and Sentinel-2 Images. In *Advances in Forest Fire Research*; Viegas, D.X., Ed.; Imprensa da Universidade de Coimbra: Coimbra, Portugal, 2018; pp. 218–226.
73. Myoung, B.; Kim, S.H.; Nghiem, S.V.; Jia, S.; Whitney, K.; Kafatos, M.C. Estimating live fuel moisture from MODIS satellite data for wildfire danger assessment in Southern California USA. *Remote Sens.* **2018**, *10*, 87. [CrossRef]

74. Marino, E.; Yebra, M.; Guillén-Climent, M.; Algeet, N.; Tomé, J.L.; Madrigal, J.; Guijarro, M.; Hernando, C. Investigating live fuel moisture content estimation in fire-prone shrubland from remote sensing using empirical modelling and RTM simulations. *Remote Sens.* **2020**, *12*, 2251. [CrossRef]
75. Costa-Saura, J.M.; Balaguer-Beser, Á.; Ruiz, L.A.; Pardo-Pascual, J.E.; Soriano-Sancho, J.L. Empirical models for spatio-temporal live fuel moisture content estimation in mixed mediterranean vegetation areas using sentinel-2 indices and meteorological data. *Remote Sens.* **2021**, *13*, 3726. [CrossRef]
76. Zhu, L.; Webb, G.I.; Yebra, M.; Scortechini, G.; Miller, L.; Petitjean, F. Live fuel moisture content estimation from MODIS: A deep learning approach. *ISPRS J. Photogramm. Remote Sens.* **2021**, *179*, 81–91. [CrossRef]
77. Miller, L.; Zhu, L.; Yebra, M.; Rüdiger, C.; Webb, G.I. Multi-modal temporal CNNs for live fuel moisture content estimation. *Environ. Model. Softw.* **2022**, *156*, 105467. [CrossRef]
78. Tanase, M.A.; Nova, J.P.G.; Marino, E.; Aponte, C.; Tomé, J.L.; Yáñez, L.; Madrigal, J.; Guijarro, M.; Hernando, C. Characterizing live fuel moisture content from active and passive sensors in a mediterranean environment. *Forests* **2022**, *13*, 1846. [CrossRef]
79. Arcos, M.A.; Edo-Botella, R.; Balaguer-Beser, Á.; Ruiz, L.Á. Analyzing independent LFMC empirical models in the mid-Mediterranean region of Spain attending to vegetation types and bioclimatic zones. *Forests* **2023**, *14*, 1299. [CrossRef]
80. Benali, A.; Baldassarre, G.; Loureiro, C.; Briquemont, F.; Fernandes, P.M.; Rossa, C.; Figueira, R. A Near-Real-Time Operational Live Fuel Moisture Content (LFMC) Product to Support Decision-Making at the National Level. *Fire* **2025**, *8*, 178. [CrossRef]
81. Wang, L.; Quan, X.; He, B.; Yebra, M.; Xing, M.; Liu, X. Assessment of the dual polarimetric sentinel-1A data for forest fuel moisture content estimation. *Remote Sens.* **2019**, *11*, 1568. [CrossRef]
82. Miller, L.; Zhu, L.; Yebra, M.; Rüdiger, C.; Webb, G.I. Projecting live fuel moisture content via deep learning. *Int. J. Wildland Fire* **2023**, *32*, 709–727. [CrossRef]
83. Pellizzaro, G.; Cesaraccio, C.; Duce, P.; Ventura, A.; Zara, P. Relationships between seasonal patterns of live fuel moisture and meteorological drought indices for Mediterranean shrubland species. *Int. J. Wildland Fire* **2007**, *16*, 232–241. [CrossRef]
84. Zhang, H.; Wu, B.; Yan, N.; Zhu, W.; Feng, X. An improved satellite-based approach for estimating vapor pressure deficit from MODIS data. *J. Geophys. Res. Atmos.* **2014**, *119*, 12256–12271. [CrossRef]
85. Kerr, Y.H.; Waldteufel, P.; Wigneron, J.-P.; Delwart, S.; Cabot, F.; Boutin, J.; Escorihuela, M.-J.; Font, J.; Reul, N.; Gruhier, C. The SMOS mission: New tool for monitoring key elements ofthe global water cycle. *Proc. IEEE* **2010**, *98*, 666–687. [CrossRef]
86. Holgate, C.; De Jeu, R.A.; van Dijk, A.I.J.M.; Liu, Y.; Renzullo, L.J.; Dharssi, I.; Parinussa, R.M.; Van Der Schalie, R.; Gevaert, A.; Walker, J. Comparison of remotely sensed and modelled soil moisture data sets across Australia. *Remote Sens. Environ.* **2016**, *186*, 479–500. [CrossRef]
87. Bhardwaj, J.; Kuleshov, Y.; Chua, Z.-W.; Watkins, A.B.; Choy, S.; Sun, Q. Evaluating satellite soil moisture datasets for drought monitoring in Australia and the South-West Pacific. *Remote Sens.* **2022**, *14*, 3971. [CrossRef]
88. Holgate, C.M.; Van DIjk, A.I.; Cary, G.J.; Yebra, M. Using alternative soil moisture estimates in the McArthur Forest Fire Danger Index. *Int. J. Wildland Fire* **2017**, *26*, 806–819. [CrossRef]
89. Merrill, D.; Alexander, M.E. *Glossary of Forest fire Management Terms*; Canadian Committee on Forest Fire Management, National Research Council of Canada: Ottawa, ON, Canada, 1987.
90. Chuvieco, E.; Riaño, D.; Van Wagtendok, J.; Morsdof, F. Fuel loads and fuel type mapping. In *Wildland Fire Danger Estimation and Mapping: The Role of Remote Sensing Data*; World Scientific: Hackensack, NJ, USA, 2003; pp. 119–142.
91. Pettinari, M.L.; Chuvieco, E. Fire danger observed from space. *Surv. Geophys.* **2020**, *41*, 1437–1459. [CrossRef]
92. Lawson, B.; Stocks, B.; Alexander, M.; Van Wagner, C. A system for predicting fire behavior in Canadian forests. In Proceedings of the Eighth Conference on Fire and Forest Meteorology, Detroit, MI, USA, 29 April–2 May 1985; Society of American Foresters: Bethesda, MA, USA, 1985.
93. Forestry Canada. *Development and Structure of the Canadian Forest Fire Behavior Prediction System*; Rep. No. ST-X-3; Forestry Canada: Ottawa, ON, Canada, 1992.
94. Arroyo, L.A.; Healey, S.P.; Cohen, W.B.; Cocero, D.; Manzanera, J.A. Using object-oriented classification and high-resolution imagery to map fuel types in a Mediterranean region. *J. Geophys. Res. Biogeosci.* **2006**, *111*, 1–10. [CrossRef]
95. Fogarty, L.; Pearce, H.; Catchpole, W.; Alexander, M. Adoption vs. adaptation: Lessons from applying the Canadian forest fire danger rating system in New Zealand. In Proceedings of the 3rd International Conference on Forest Fire Research and 14th Fire and Forest Meteorology Conference, Luso, Coimbra, Portugal, 16–20 November 1998.
96. Leonardo, E.M.C.; Watt, M.S.; Pearse, G.D.; Dash, J.P.; Persson, H.J. Comparison of TanDEM-X InSAR data and high-density ALS for the prediction of forest inventory attributes in plantation forests with steep terrain. *Remote Sens. Environ.* **2020**, *246*, 111833. [CrossRef]
97. Mallinis, G.; Galidaki, G.; Gitas, I. A comparative analysis of EO-1 Hyperion, Quickbird and Landsat TM imagery for fuel type mapping of a typical Mediterranean landscape. *Remote Sens.* **2014**, *6*, 1684–1704. [CrossRef]

98. Roberts, D.A.; Dennison, P.E.; Gardner, M.E.; Hetzel, Y.; Ustin, S.L.; Lee, C.T. Evaluation of the potential of Hyperion for fire danger assessment by comparison to the Airborne Visible/Infrared Imaging Spectrometer. *IEEE Trans. Geosci. Remote Sens.* **2003**, *41*, 1297–1310. [CrossRef]
99. Mutlu, M.; Popescu, S.C.; Stripling, C.; Spencer, T. Mapping surface fuel models using lidar and multispectral data fusion for fire behavior. *Remote Sens. Environ.* **2008**, *112*, 274–285. [CrossRef]
100. Varga, T.A.; Asner, G.P. Hyperspectral and LiDAR remote sensing of fire fuels in Hawaii Volcanoes National Park. *Ecol. Appl.* **2008**, *18*, 613–623. [CrossRef]
101. Chrysafis, I.; Damianidis, C.; Giannakopoulos, V.; Mitsopoulos, I.; Dokas, I.M.; Mallinis, G. Vegetation Fuel Mapping at Regional Scale Using Sentinel-1, Sentinel-2, and DEM Derivatives—The Case of the Region of East Macedonia and Thrace, Greece. *Remote Sens.* **2023**, *15*, 1015. [CrossRef]
102. Riaño, D.; Chuvieco, E.; Salas, J.; Palacios-Orueta, A.; Bastarrika, A. Generation of fuel type maps from Landsat TM images and ancillary data in Mediterranean ecosystems. *Can. J. For. Res.* **2002**, *32*, 1301–1315. [CrossRef]
103. Hardy, C.C.; Burgan, R.E. Evaluation of NDVI for monitoring live moisture in three vegetation types of the western US. *Photogramm. Eng. Remote Sens.* **1999**, *65*, 603–610.
104. Cunill Camprubi, A.; González-Moreno, P.; Resco de Dios, V. Live fuel moisture content mapping in the Mediterranean Basin using random forests and combining MODIS spectral and thermal data. *Remote Sens.* **2022**, *14*, 3162. [CrossRef]
105. Arganaraz, J.P.; Landi, M.A.; Bravo, S.J.; Gavier-Pizarro, G.I.; Scavuzzo, C.M.; Bellis, L.M. Estimation of live fuel moisture content from MODIS images for fire danger assessment in Southern Gran Chaco. *IEEE J. Sel. Top. Appl. Earth Obs. Remote Sens.* **2016**, *9*, 5339–5349. [CrossRef]
106. Lai, G.; Quan, X.; Yebra, M.; He, B. Model-driven estimation of closed and open shrublands live fuel moisture content. *GIScience Remote Sens.* **2022**, *59*, 1837–1856. [CrossRef]
107. Riaño, D.; Vaughan, P.; Chuvieco, E.; Zarco-Tejada, P.J.; Ustin, S.L. Estimation of fuel moisture content by inversion of radiative transfer models to simulate equivalent water thickness and dry matter content: Analysis at leaf and canopy level. *IEEE Trans. Geosci. Remote Sens.* **2005**, *43*, 819–826. [CrossRef]
108. DeCastro, A.L.; Juliano, T.W.; Kosović, B.; Ebrahimian, H.; Balch, J.K. A computationally efficient method for updating fuel inputs for wildfire behavior models using sentinel imagery and random forest classification. *Remote Sens.* **2022**, *14*, 1447. [CrossRef]
109. Palomino, A.F.; Espino, P.S.; Reyes, C.B.; Rojas, J.A.J.; y Silva, F.R. Estimation of moisture in live fuels in the mediterranean: Linear regressions and random forests. *J. Environ. Manag.* **2022**, *322*, 116069. [CrossRef]
110. Adab, H.; Devi Kanniah, K.; Beringer, J. Estimating and Up-Scaling Fuel Moisture and Leaf Dry Matter Content of a Temperate Humid Forest Using Multi Resolution Remote Sensing Data. *Remote Sens.* **2016**, *8*, 961. [CrossRef]
111. Yebra, M.; Quan, X.; Riaño, D.; Larraondo, P.R.; Van Dijk, A.I.; Cary, G.J. A fuel moisture content and flammability monitoring methodology for continental Australia based on optical remote sensing. *Remote Sens. Environ.* **2018**, *212*, 260–272. [CrossRef]
112. Yebra, M.; Shokirov, S. *Validation of Fuel Moisture Content Estimates from the Australian Flammability Monitoring Systems for Coastal Shrublands in the Perth Region—Black Summer Final Report*; Bushfire and Natural Hazards CRC: Melbourne, Australia, 2022.
113. Quan, X.; Yebra, M.; Riaño, D.; He, B.; Lai, G.; Liu, X. Global fuel moisture content mapping from MODIS. *Int. J. Appl. Earth Obs. Geoinf.* **2021**, *101*, 102354. [CrossRef]
114. Trouvé, R.; Jiang, R.; Fedrigo, M.; White, M.D.; Kasel, S.; Baker, P.J.; Nitschke, C.R. Combining environmental, multispectral, and LiDAR data improves forest type classification: A case study on mapping cool temperate rainforests and mixed forests. *Remote Sens.* **2022**, *15*, 60. [CrossRef]
115. Long, X.; Li, X.; Lin, H.; Zhang, M. Mapping the vegetation distribution and dynamics of a wetland using adaptive-stacking and Google Earth Engine based on multi-source remote sensing data. *Int. J. Appl. Earth Obs. Geoinf.* **2021**, *102*, 102453. [CrossRef]
116. Pande-Chhetri, R.; Abd-Elrahman, A.; Liu, T.; Morton, J.; Wilhelm, V.L. Object-based classification of wetland vegetation using very high-resolution unmanned air system imagery. *Eur. J. Remote Sens.* **2017**, *50*, 564–576. [CrossRef]
117. Degerickx, J.; Roberts, D.A.; Somers, B. Enhancing the performance of Multiple Endmember Spectral Mixture Analysis (MESMA) for urban land cover mapping using airborne lidar data and band selection. *Remote Sens. Environ.* **2019**, *221*, 260–273. [CrossRef]
118. Malhi, R.K.M.; Kiran, G.S.; Srivastava, P.K.; Bhattacharya, B.K.; Mohanta, A. Spectral mixture analysis of AVIRIS-NG data for grouping plant functional types. *Adv. Space Res.* **2024**, *73*, 1439–1448. [CrossRef]
119. Zheng, J.-Y.; Hao, Y.-Y.; Wang, Y.-C.; Zhou, S.-Q.; Wu, W.-B.; Yuan, Q.; Gao, Y.; Guo, H.-Q.; Cai, X.-X.; Zhao, B. Coastal Wetland Vegetation Classification Using Pixel-Based, Object-Based and Deep Learning Methods Based on RGB-UAV. *Land* **2022**, *11*, 2039. [CrossRef]
120. McArthur, A.G. *Fire Behaviour in Eucalypt Forests*; Forestry and Timber Bureau Leaflet 107; Forestry and Timber Bureau, Department of National Development: Canberra, ACT, Australia, 1967.
121. Rothermel, R.C. *A Mathematical Model for Predicting Fire Spread in Wildland Fuels*; Research Paper INT-115; Intermountain Forest & Range Experiment Station, Forest Service, US Department of Agriculture: Ogden, UT, USA, 1972; Volume 115.
122. Papadopoulos, G.D.; Pavlidou, F.-N. A comparative review on wildfire simulators. *IEEE Syst. J.* **2011**, *5*, 233–243. [CrossRef]

123. Singh, H.; Ang, L.-M.; Paudyal, D.; Acuna, M.; Srivastava, P.K.; Srivastava, S.K. A Comprehensive Review of Empirical and Dynamic Wildfire Simulators and Machine Learning Techniques used for the Prediction of Wildfire in Australia. *Technol. Knowl. Learn.* **2025**, *30*, 935–968. [CrossRef]
124. Anderson, S.A.J.; Schou, W.C.; Clement, B. *NZ Fire Behaviour Toolkit: User Guide and Technical Report*; New Zealand Fire Service Commission Research Report #105; New Zealand Fire Service Commission: Wellington, New Zealand, 2008; ISBN 978-1-877539-21-3.
125. Tymstra, C.; Bryce, R.W.; Wotton, B.M.; Taylor, S.W.; Armitage, O.B. *Development and Structure of Prometheus: The Canadian Wildland Fire Growth Simulation Model*; Information Report NOR-X-417; Natural Resources Canada, Canadian Forest Service, Northern Forestry Centre: Edmonton, AB, Canada, 2010; 88p.
126. Thompson, S.; Grüner, I.; Gapare, N. *New Zealand Land Cover Database Version 2: Illustrated Guide to Target Classes*; Ministry for the Environment: Wellington, New Zealand, 2003.
127. Landcare Research. *LCDB v5.0—Land Cover Database Version 5.0*; Landcare Research New Zealand Ltd.: Mainland, New Zealand, 2020. Available online: https://lris.scinfo.org.nz/layer/104400-lcdb-v50-land-cover-database-version-50-mainland-new-zealand-deprecated/ (accessed on 15 August 2025).
128. Fire and Emergency New Zealand (FENZ). *Grassland Curing Guide: New Zealand Edition*; Fire and Emergency New Zealand: Wellington, New Zealand, 2023.
129. Anderson, S.A.J. Future Options for Fire Behaviour Modelling and Fire Danger Rating in New Zealand. *Proc. R. Soc. Qld.* **2009**, *115*, 119–127. [CrossRef]
130. Wiser, S.; Arnst, E. NZ National Vegetation Survey Occurrence Data. Landcare Research. Occurrence Dataset. 2025. Available online: https://www.gbif.org/dataset/788439f0-3b56-11dc-8c19-b8a03c50a862 (accessed on 24 September 2025).
131. Guk, E.; Bar-Massada, A.; Yebra, M.; Scortechini, G.; Levin, N. Examining the Transferability of Remote-Sensing-Based Models of Live Fuel Moisture Content for Predicting Wildfire Characteristics. *IEEE J. Sel. Top. Appl. Earth Obs. Remote Sens.* **2024**, *17*, 14762–14776. [CrossRef]
132. CSIRO. SPARK: A Toolkit for the End-to-End Processing, Simulation and Analysis of Wildfires. 2024. Available online: https://research.csiro.au/spark/ (accessed on 16 August 2025).
133. Tolhurst, K.; Shields, B.; Chong, D. Phoenix: Development and application of a bushfire risk management tool. *Aust. J. Emerg. Manag.* **2008**, *23*, 47–54.
134. McGrattan, K.; Hostikka, S.; McDermott, R.; Floyd, J.; Weinschenk, C.; Overholt, K. *Fire Dynamics Simulator FDS User's Guide*; NIST Special Publication 1018-5; National Institute of Standards and Technology: Gaithersburg, MD, USA, 2014.
135. Finney, M.A.; Andrews, P.L. FARSITE: Fire Area Simulator—A program for fire growth simulation. *Fire Manag. Notes* **1999**, *59*, 13–15.
136. Finney, M.A. An overview of FlamMap fire modeling capabilities. In *Fuels Management-How to Measure Success: Conference Proceedings, Portland, OR, USA, 28–30 March 2006*; Proceedings RMRS-P-41; Andrews, P.L., Butler, B.W., Eds.; USDA Forest Service, Rocky Mountain Research Station: Fort Collins, CO, USA, 2006; pp. 213–220.
137. Dillon, G.K.; Scott, J.H.; Jaffe, M.R.; Olszewski, J.H.; Vogler, K.C.; Finney, M.A.; Short, K.C.; Riley, K.L.; Grenfell, I.C.; Jolly, W.M.; et al. *Spatial Datasets of Probabilistic Wildfire Risk Components for the United States (270 m)*, 3rd ed.; Forest Service Research Data Archive: Fort Collins, CO, USA, 2023. [CrossRef]
138. Cimdins, R.; Krasovskiy, A.; Kraxner, F. Regional Variability and Driving Forces behind Forest Fires in Sweden. *Remote Sens.* **2022**, *14*, 5826. [CrossRef]

Disclaimer/Publisher's Note: The statements, opinions and data contained in all publications are solely those of the individual author(s) and contributor(s) and not of MDPI and/or the editor(s). MDPI and/or the editor(s) disclaim responsibility for any injury to people or property resulting from any ideas, methods, instructions or products referred to in the content.